


PHYSICS ASPECTS OF THE COMPACT IGNITION TOKAMAK

By

D. Post et al.

NOVEMBER 1986

PLASMA
PHYSICS
LABORATORY 

PRINCETON UNIVERSITY
PRINCETON, NEW JERSEY

PREPARED FOR THE U.S. DEPARTMENT OF ENERGY,
UNDER CONTRACT DE-AC82-76-CED-3073.

DISCLAIMER

This report was prepared as an account of work sponsored by an agency of the United States Government. Neither the United States Government nor any agency thereof, nor any of their employees, makes any warranty, express or implied, or assumes any legal liability or responsibility for the accuracy, completeness, or usefulness of any information, apparatus, product, or process disclosed, or represents that its use would not infringe privately owned rights. Reference herein to any specific commercial product, process, or service by trade name, trademark, manufacturer, or otherwise does not necessarily constitute or imply its endorsement, recommendation, or favoring by the United States Government or any agency thereof. The views and opinions of authors expressed herein do not necessarily state or reflect those of the United States Government or any agency thereof.

PHYSICS ASPECTS OF THE COMPACT IGNITION TOKAMAK

D. Post,¹ G. Bateman,¹ W. Houlberg,² L. Bromberg,³ D. Cohn,³
 P. Colestock,¹ M. Hughes,⁴ D. Ignat,¹ R. Izzo,¹ S. Jardin,¹
 C. Kieras-Phillips,¹ L.P. Ku,¹ G. Kuo-Petravic,¹ B. Lipschultz,³
 R. Parker,³ C. Paulson,⁴ Y-K. M. Peng,⁵ M. Petravic,¹
 M. Phillips,⁴ N. Pomphrey,¹ J. Schmidt,¹ D. Strickler,⁵
 A. Todd,⁴ N. Uckan,² R. White,¹ S. Wolfe,³ and K. Young¹

/ Plasma Physics Laboratory, Princeton University
 Princeton, NJ 08544 USA

ABSTRACT

The Compact Ignition Tokamak (CIT) is a proposed modest-size ignition experiment designed to study the physics of alpha-particle heating. The basic concept is to achieve ignition in a modest-size minimum cost experiment by using a high plasma density to achieve the condition of $n\tau_E \sim 2 \times 10^{20} \text{ sec m}^{-3}$ required for ignition. The high density requires a high toroidal field (10 T). The high toroidal field allows a large plasma current (10 MA) which improves the energy confinement, and provides a high level of ohmic heating. The present CIT design also has a high degree of elongation ($\kappa \sim 1.8$) to aid in producing the large plasma current. A double null poloidal divertor and a pellet injector are part of the design to provide impurity and particle control, improve the confinement, and provide flexibility for improving the plasma profiles. Since auxiliary heating is expected to be necessary to achieve ignition, 10-20 MW of Ion Cyclotron Radio Frequency (ICRF) is to be provided.

¹Princeton Plasma Physics Laboratory, Princeton, NJ.

²Oak Ridge National Laboratory, Oak Ridge, TN.

³Massachusetts Institute of Technology, Cambridge, MA.

⁴Grumman Aerospace Corporation, Princeton, NJ.

⁵Fusion Engineering Design Center, Oak Ridge, TN.

MASTER

DISTRIBUTION OF THIS DOCUMENT IS UNLIMITED

CONTENTS

1.	INTRODUCTION.....	3
1.1	Background.....	3
1.2	Physics Objectives.....	5
2.	PHYSICS REQUIREMENTS, DESIGN CONSTRAINTS, AND OPERATIONAL LIMITS.....	6
2.1	Physics Requirements.....	6
2.2	Discharge Parameters and Operational Limits.....	10
2.3	Discharge Scenarios.....	10
3.	ENERGY CONFINEMENT.....	11
3.1	Characterization of Energy Confinement.....	11
3.2	Confinement Projections for CIT.....	13
4.	PROJECTIONS OF CIT PLASMA PERFORMANCE.....	15
4.1	Start-up.....	15
4.2	Auxiliary Heating and Ignition.....	17
4.3	Burn.....	19
4.4	Shutdown.....	21
5.	AUXILIARY HEATING.....	21
5.1	Summary of the Experiment Data.....	22
5.2	ICRF Heating Strategy for CIT.....	23
5.3	Antenna Physics.....	24
6.	MAGNETICS.....	25
6.1	Axisymmetric Magnetics.....	25
6.2	Beta Limits.....	26
6.3	Fishbone Instabilities.....	27
7.	IMPURITY AND PARTICLE CONTROL.....	28
7.1	Plasma Edge Characteristics.....	28
7.2	Divertor Operation.....	29
7.3	Limiter Operation.....	31
7.4	Density Control and Fueling.....	31
7.5	Disruptions.....	32
8.	DIAGNOSTICS AND OPERATIONS.....	33
8.1	Operations.....	33
8.2	Diagnostics.....	33
9.	SUMMARY.....	34
	ACKNOWLEDGMENTS.....	34
	REFERENCES.....	36
	TABLES.....	37
	FIGURES.....	47

1.0 INTRODUCTION

1.1 Background

There has been substantial progress in fusion research, especially tokamaks, in the last two decades. The earliest tokamak experiments (T-3, ST) in the late 1960s and early 1970s have been succeeded by successively larger experiments (ATC, ORMAK, TFR, PLT, T-4, T-10, T-11, PDX, D-II, D-III, Pulsator, DITE, PDX, JFT-II, JIPT-II) culminating in the three large experiments now operating (TFTR, JET, and JT-60). This progress is illustrated in the steady improvement of density times confinement time ($n\tau$) (Fig. 1) and other tokamak parameters. A comparison of the best plasma parameters achieved by one of the earliest experiments (ST)¹ and those recently achieved show that the improvement in each parameter has generally been between one and two orders of magnitude (Table 1). The best parameters are close to those required for a fusion reactor ($T \sim 15$ keV, $n\tau \sim 2-3 \times 10^{20}$ sec m⁻³, $\tau_E \sim 1-2$ sec, $\beta \sim 7-10\%$, and $Z_{\text{eff}} \sim 1.5-2$). Previous plans for the development of fusion energy called for the construction of a large, ignited tokamak reactor experiment to be operated in the mid-1990's to develop and test both the physics and technology basis for a commercial fusion reactor. In the U.S., this class of experiment has been embodied in the INTOR and Fusion Engineering Device (FED) studies and the ongoing Engineering Test Reactor (ETR) studies.

However, there have been three developments in the U.S. which have led to interest in constructing and operating a smaller-scale ignition physics experiment, an experiment which is cheaper than an INTOR class experiment, and one which can investigate the physics of ignition. The first development is related to the energy confinement in recent experiments. While the energy confinement times in experiments with high-power auxiliary heating, such as TFTR and JET, are within factors of 2 to 6 of those needed for a reactor, the energy confinement appears to deteriorate gradually as the level of auxiliary heating is increased. If this trend continues with the high levels of alpha-particle heating needed for an ignited plasma, the presently envisaged ETR experiment designs will have to be extensively modified. Thus, the effectiveness of alpha-particle heating and its effect on confinement is a key issue for future ignited tokamak experiments.

The second issue is the public perception in the U.S. that it is now less urgent than previously thought in the late 1970s to accelerate research to

develop alternate energy sources. This has meant a severe curtailment of such programs as solar power and syn-fuels. For fusion, this has meant that, in the opinion of the U.S. government, the time scale for a multi-billion dollar fusion experiment funded exclusively by the U.S. may have to be postponed into the late 1990s.

The third event has been the development of a feasible concept for an inexpensive, compact ignition experiment, based upon the use of high toroidal fields and high densities embodied in the Alcator experiments at the Massachusetts Institute of Technology (MIT), to achieve the required $n\tau$ of $2-3 \times 10^{20}$ sec m^{-3} for ignition in a compact and relatively inexpensive experiment. This type of concept has an extensive history. The idea of using a high field (10 T), small ($R = 1.4$ m), ohmically heated experiment was discussed by Kadomtsev and Pogutse in 1967,² and also in the 1970s.³⁻⁵ In the late 1970s, a group at IPP, Garching seriously proposed building such a compact ignition experiment, ZEPHYR, but the proposal was not funded.

These three developments have led to the proposal of the Compact Ignition Tokamak (CIT) experiment. The role of this experiment would be to explore the physics of ignited plasmas, particularly, alpha-particle heating. Given the reduced funding level available for large-scale fusion experiments, it will have to be relatively inexpensive and not require large increases in the total fusion budget. These constraints can be met with a small, high-field experiment of the general class described above.

The choice of a compact high-field experiment has led to a design using liquid-nitrogen-cooled copper coils. Resistive heating of the coils limits the pulse length to ~5 sec in the current design. The high fields lead to high-stress levels in the coils. The stresses will be reduced with a hydraulic press. The crack growth due to fatigue leads, in combination with radiation damage of the coil insulation, to a relatively small number of full-power pulses (~3,000) with D-T and a larger number of half stress pulses (~50,000). The machine parameters are listed in Table 2. The CIT will require auxiliary heating, and 10-20 MW of ICRF is planned. Impurity control will be provided by both an inside bumper limiter, and a double null poloidal divertor. Fueling will be accomplished with both gas injection and repeating pellet injection systems. Protection of the vacuum vessel will be accomplished with a layer of carbon tiles covering the entire vacuum vessel wall. The carbon tiles and other internal hardware will be maintained with

remote handling techniques.

1.2 Physics Objectives

The objective of the CIT is to provide the physical information which is necessary for designing an engineering test reactor and which cannot be obtained from the present generation of large tokamak experiments. The CIT is primarily an "alpha-particle" heating experiment which will concentrate on the physics issues associated with ignition and burn, with the synergism between the presence of a significant density of high-energy alpha particles, and the basic physics performance factors for tokamak discharges, such as confinement and beta limits.

The effectiveness of alpha-particle heating and its impact on confinement and beta limits is the major issue for CIT. Classical models show that alpha-particle heating is strongly peaked in the plasma center and primarily heats the electrons.^{6,7} It would thus be expected to alter the density and temperature profiles, as well as affect the behavior of sawtooth oscillations. The profile modifications and other effects could likely lead to changes in the beta limits and confinement times. While some information on these effects would be available for subignited plasmas (Q 's of 5-10), their full study demands an ignited plasma. Since these effects have time scales of the order of the energy confinement time, a burn pulse length of $10\tau_E$ should be adequate for their study.

The confinement and slowing down of single alpha particles is not expected to be an important issue for CIT and probably will be resolved on the Joint European Torus (JET) and the Tokamak Fusion Test Reactor (TFTR). However, there are a number of questions that involve the potential interaction of an energetic-alpha-particle population having a finite density and pressure with the background plasma. The energetic-alpha-particle population may cause microinstabilities which could lead to anomalous slowing down, transport, or loss of fast alphas.⁸ The fast-alpha population could also affect the macrostability of the plasma leading to instabilities, such as "fishbones," which would then lead to loss of the energetic alphas. The relatively large orbits of the fast alphas and their prompt loss may lead to substantial radial electric fields and plasma rotation. The fast alphas are also expected to increase the ablation rate of pellets.⁹ These questions can be addressed with an ignited and burning plasma, and could likely be addressed

with a subignited plasma with $Q > 5$.

Control of an ignited plasma will be studied on CIT. The question as to what phenomena determine the upper limits on the burn is a major objective of the CIT experiment. Possible limits may be due to the "soft" beta limits, confinement degradation with nonohmic heating power, and radiation losses. CIT will provide an opportunity to test "active" as well as passive burn control techniques.

The CIT is potentially capable of exploring new parameter ranges and contributing to the understanding of energy and particle confinement, the effectiveness of radio-frequency heating, the control and stability of highly elongated low- q , high-beta plasmas, disruptions, fueling, and impurity control with high-heat fluxes.

Making substantial contributions to the understanding of the physics of ignited plasmas requires a well planned set of diagnostics capable of withstanding the radiation environment. These diagnostics have to be built into the CIT design. Detailed measurements are required of the plasma parameters and profiles, and provision has to be made for alpha-particle diagnostics.

2.0 PHYSICS REQUIREMENTS, DESIGN CONSTRAINTS, AND OPERATIONAL LIMITS

2.1 Physics Requirements

The physics requirements for the CIT have been derived from the mission of achieving ignition with the added constraint of low cost and, therefore, compact size. Those objectives, combined with realizable engineering technology, lead to a device with high magnetic fields, large plasma currents, and high fusion power densities. Ignition requires an $n\tau_E$ of about 2×10^{20} sec m^{-3} . With modest size (and thus modest τ_E) this can be achieved with high densities, which require high toroidal fields. The high density implies that the fusion power density will be high. The high toroidal field also allows a high plasma current, which can keep the beta in the 5-6% range,¹⁰ to increased energy confinement times (τ_E),¹¹ and to significant levels of ohmic heating. The plasma current is increased further by elongating the plasma. To reach a high enough temperature for ignition, the ohmic heating must be supplemented by auxiliary heating. A poloidal divertor and pellet injection system have been made part of the CIT design to provide a margin for confinement and $n\tau_E$ and to provide impurity and particle control.

The basic CIT physics guidelines (Table 3) have been established by the Ignition Technical Oversight Committee (ITOC), the Ignition Physics Study Group (IPSG), and the CIT physics design team. The ITOC, composed of senior-level physicists representing all of the major groups in the magnetic fusion community, set the general CIT guidelines after consideration of the relevant issues. The IPSG, composed of about 100 working physicists (experimentalists, theorists, and modelers) drawn from the fusion laboratories and university groups, gave guidance on the physics issues for CIT. Panel XIV, formed by the Magnetic Fusion Advisory Committee, helped to formulate the goals for CIT. The CIT physics design team then translated the general physics guidelines, reflecting both operational experience on tokamak experiments and the best available tokamak theory.

The confinement guidelines are based upon consideration of the various scalings laws developed from present tokamak experiments.¹² The requirement is for CIT to achieve ignition using extrapolations of a reasonable range of these scaling laws and properly designed operational scenarios. Energy confinement in present experiments can be characterized as falling into the three general classes depending on, among other things, the heating method: ohmic heating, auxiliary heating with limiters (L-mode),¹¹ and auxiliary heating with divertors (H-mode).¹³ While the confinement time with the ohmic heating scalings is adequate for ignition, the temperature with ohmic heating is too low for ignition and auxiliary heating is required to raise the temperature to ignition conditions. The use of high-power auxiliary heating in tokamaks has been observed to reduce the confinement time to values below the value with ohmic heating alone (L-mode). The degraded L-mode confinement time can be increased by operation with a poloidal divertor (H-mode), and it is partly for this reason that a divertor is part of the CIT design. In addition, experiments indicate that pellet fueling can produce centrally peaked density profiles which facilitate ignition by increasing the central fusion reaction rate and the confinement time. Thus, pellet fueling is also part of the CIT design. Pellet fueling and a divertor will provide two levels of added insurance against the more pessimistic L-mode scaling. To assure that the CIT is designed to meet the requirement of ignition, it is assumed that alpha heating produces the same level of confinement degradation as auxiliary heating. Since a poloidal divertor is part of the CIT design, the requirement for ignition refers to H-mode confinement as the CIT

"reference" case, but profile control with pellet fueling should allow ignition with L-mode confinement.

These confinement considerations can be characterized by an approximate figure of merit $X = aB_T^2/q_{cyl}$, which is proportional to the ignition "margin" P_α/P_{Loss} at a fixed temperature, and which is computed at the maximum density and beta for a standard ohmic-heating energy-confinement scaling (neo-Alcator).¹⁴ The ignition margin with auxiliary-heating confinement scaling improves with increasing X . A value of X equal to or greater than 25 has been specified for the design.

The volume-averaged density limit is assumed to be given by the Murakami-Hugill limit.¹⁵ This is a conservative limit since there are experiments with pellet fueling which show that this limit can be exceeded. In addition, other recent scalings, such as the one developed by M. Greenwald as part of the IPSC studies, indicate that the high elongation of CIT may increase the density limit above the Murakami-Hugill limit.

A beta limit of the Troyon-Gruber¹⁰ form (appropriate for the CIT plasma shape) was chosen since this type of limit correlates well with present experiments and detailed calculations. A conservative coefficient (3.0) was chosen to minimize the disruption frequency, even though coefficients of 3.5 for long pulses and 4.0 on a transient basis are consistent with the best results achieved in experiments.

The plasma shape is limited to elongations $\kappa \leq 1.8$ and aspect ratios (R/a) around 2.7. The elongation limit was set to avoid plasma control problems with the vertical instabilities usually associated with high elongations. Our study of this issue indicates that this elongation is achievable, and that even larger elongations (perhaps up to 2.5) are also feasible.

A design plasma current of 10-MA for limiter operation has been chosen to achieve high plasma pressures, to allow substantial ohmic heating, and to maximize the confinement with auxiliary heating. For divertor operation the achievable plasma current will be at least 9-MA. Higher plasma currents will be achievable with the divertor at a reduced MHD safety factor q . The plasma current is constrained by the requirement that the MHD safety factor at the plasma edge, q , be greater than 2.6 and with an additional requirement that the $q = 2$ surface be at least 5 cm inside the plasma boundary. These constraints were set to avoid disruptions and reflect operational experience

on tokamaks with divertors. There are some indications, primarily from the Poloidal Divertor Experiment (PDX), that these requirements are conservative and that lower q 's may be obtainable.

The burn duration at maximum current and field is required to be about 10 energy-confinement times (τ_E) at 10 keV, to allow time to study the physics of alpha-particle heating. The τ_E is much greater than the alpha-particle slowing down time, but much less than the resistive skin time. An additional $2\tau_E$ of toroidal field flattop is specified to allow for heating to ignition, which will be initiated during the field ramp-up. A confinement time of about one-third of a second is required to achieve ignition. A typical discharge scenario is expected to consist of ~3.0 sec of current ramp-up during which auxiliary heating is started ~4 sec of auxiliary heating and burn, and 2-3 sec for discharge termination and shutdown.

There will be substantial levels of ohmic heating due to the high plasma current densities achievable in CIT. However, auxiliary heating is required for ignition even using the best values of ohmic-heating confinement times. The amount of auxiliary heating power required to augment the ohmic heating to achieve ignition depends on the confinement time for CIT. Initially, 10 MW of heating is to be provided which is adequate for ignition if the confinement follows some of the more optimistic confinement time scalings. However, the experiment is designed to handle 20 MW of auxiliary heating should it prove necessary. Twenty megawatts of auxiliary heating should be adequate to achieve ignition with the confinement times predicted for divertor operation using the H-mode scalings for L-mode scalings if the density profile is peaked with pellet fueling. This heating should also be adequate to obtain substantial alpha heating ($Q \geq 10$) if the confinement follows some of the most pessimistic L-mode, scalings and no credit is taken for the divertor and pellet fueling. Ion Cyclotron Radio-Frequency (ICRF) heating is to be the reference heating method. Ion cyclotron radio-frequency heating has been quite successful in recent experiments¹⁶ and provides a number of technical advantages over other heating techniques. Switching to another promising heating technique, such as electron cyclotron radio-frequency (ECRF), will also be possible if one of these techniques proves successful in planned experiments and offers either physics or engineering advantages compared to ICRF.

Impurity control is to be accomplished with an inside bumper limiter and a double null poloidal divertor. A target of $Z_{\text{eff}} \leq 1.5$ has been set based on the good operation of present experiments. The limiter is required for start-up, ramp-down, and disruption control, and it can be used instead of the divertor during burn. The poloidal divertor is designed to localize the neutral recycling in the divertor chamber. Both the limiter and divertor are to be designed to handle the expected particle and heat fluxes, but particle removal by divertor chamber pumping is not a feature of the present design.

The minimum number of full-power burn pulses has been set to 3,000, but the experiment should be capable of operating 50,000 pulses at 70% of the full-rated field and current. This limit is set by fatigue stress limits in the coils.

2.2 Discharge Parameters and Operational Limits

Following the guidelines for the CIT Physics Basis (Table 3), a set of plasma parameters for the CIT was developed (Table 4). These parameters serve as a part of the specifications for the engineering design. The operational limits, such as the volume-averaged density, beta, elongation, and q_{ψ} , have been chosen to be conservative by the criteria developed by the IPSPG to allow some margin for tokamak operation. Other parameters, such as the radial scrape-off decay length for the power operating temperature, fusion power, and power balance, are the result of analyses of the existing experimental data and extrapolations using the best available theory.

2.3 Discharge Scenarios

A typical CIT plasma discharge will have four phases: a ramp-up phase in which the current and toroidal field are raised to their full values, an auxiliary-heating phase during which the plasma is heated to ignition, a burn phase ($\sim 10\tau_E$) during which the ignited plasma is studied, and a shutdown phase during which the current and field are ramped down. An expected ignition pulse for CIT is illustrated schematically in Fig. 2. The current and field are ramped up to their full values in a little over 3 sec. The auxiliary heating is turned on near the end of the ramp-up phase [when $B_T = 85\%$ of $B_T(\text{max})$]. After $2-3\tau_E$ of auxiliary heating, ignition occurs, and the auxiliary heating is turned off. The ignited plasma burns for approximately $10\tau_E$, and then the plasma current and field are ramped down in about 2 sec.

This scenario helps define some of the physics issues important for the successful operation of the CIT. The current must be ramped up quickly (~3 MA/sec) so that there is minimal resistive heating of the toroidal field coils during ramp-up. The confinement must be adequate to achieve ignition parameters with reasonable levels of auxiliary-heating power. The plasma must be controlled during the burn pulse, and the discharge termination must be rapid (~2 sec).

The major physics issues for the CIT design and operation are confinement, the discharge scenario, auxiliary heating, magnetics, impurity control, and operations. The crucial questions in each of these issues have been the subjects of detailed studies which are summarized in the following sections.

3.0 ENERGY CONFINEMENT

Since ignition is a goal for CIT, and ignition requires an adequate level of confinement, energy confinement is a key issue for CIT. Ignition for CIT requires a confinement time of ~200-350 msec, depending upon the density and temperature profiles. A model of this confinement is necessary for predicting the plasma parameters for CIT operation. An assessment of the present state of understanding of tokamak confinement experiments and theory was made by a subgroup of the Ignition Physics Study Group (IPSG) that included representation from all of the U.S. and many of the major foreign tokamak facilities. Energy confinement in tokamaks has generally fallen into two classes: confinement with ohmic heating and confinement with auxiliary heating. Confinement with auxiliary heating is observed to decrease as the level of auxiliary-heating power is increased. Confinement with auxiliary heating can be further subdivided into two classes, L-mode and H-mode, depending on the extent of the degradation of the confinement with auxiliary heating.

3.1 Characterization of Energy Confinement

There has been extensive experience (about a quarter of a century) along with well-established empirical scaling laws (from the TFTR, JET, Alcator-C and A, D-III and T-11 groups; regression fits by Pfeiffer and Waltz, the Alcator group, Goldston, and the D-III/JET group) for confinement with ohmic heating. At low densities and moderate q values, the data is fairly well represented by "neo-Alcator" scaling¹⁷

$$\tau_E \sim 0.07 n(10^{20} \text{ m}^{-3}) a(m) n_0^2(m) q_{\text{cyI}} \text{ (sec)}.$$

There is evidence of saturation of energy confinement at high densities, but experiments on Alcator-C, ASDEX, and TFTR indicate that this saturation can be reduced or avoided by the use of pellet fueling.¹⁸ The energy losses at low densities are, in general, dominated by electron thermal conduction. The saturation of τ_E at higher densities, in many cases, can be explained by enhanced-ion losses (instabilities driven by gradients in the ion temperature are a possible candidate), but additional electron losses cannot be ruled out. Transport models based on drift-wave turbulence are consistent with much of the observed anomalous electron confinement in the region between the $q = 1$ and $q = 2$ surfaces, but a satisfactory model does not yet exist. Although the measured density fluctuation level (\bar{n}/n) is large enough to explain the loss rate, the correlation between theory and experiment is weak.

The ion-energy confinement is generally observed to be approximately the same magnitude as predicted by neoclassical conductivity. However, in some cases (D-III), a large divergence from the neoclassical (Chang-Hinton) value has been observed in which $\chi_i \geq \chi_e$. This again may suggest the presence of nonclassical mechanisms such as ion-temperature gradient-driven modes and convective cells (in which case the magnitudes of χ_i and χ_e would be similar).

The confinement time with auxiliary heating is observed to decrease with increasing levels of auxiliary-heating power. There are many empirical scalings based on reasonable (intra- or intermachine) fits to the experimental data, mainly involving low-density ($\bar{n} \leq 10^{20} \text{ m}^{-3}$), low-current ($I \leq \text{few MA}$), and neutral-beam-heated discharges. The general form of these scalings for the energy confinement time τ_E is

$$\tau_{E,\text{aux}} \sim L I \kappa^{0.5} f(P),$$

where L is the plasma scale length ($L \sim a$ or R), I is the plasma current, κ is the elongation, and $f(P)$ represents the functional form of power degradation, which is either in the form of power law

$$f(P) \sim P^{-\alpha}; \quad \alpha \sim 1/3 - 2/3,$$

or, in an offset linear form

$$f(P) \sim C_1 + C_2/P .$$

There are two classes of confinement observed with auxiliary heating, L-mode and H-mode.

L-mode. There is an extensive data base with good reproducibility indicating that the L-regime is a universal confinement mode of auxiliary-heated tokamak plasmas, independent of specific geometry (circular/noncircular, limiter/divertor, etc.) and heating method. A wide range of empirical scaling laws have been derived from various tokamaks (intramachine scalings) using either (a) power law fits or (b) offset linear fits.¹¹ A large number of regression fits (~10) to sets of experimental data have also been derived using data sets collected from many different machines. The energy losses in the L-mode are typically dominated by electron thermal conduction. Drift-wave models reproduce some of the effects observed in L-mode scaling. There is not yet a well enough formulated theory to favor any one of the various empirical fits as more likely to be correct than any other for extrapolation to CIT.

H-mode. The H-mode, discovered on the ASDEX tokamak¹³ and confirmed by experiments on D-III, PDX, and PBX, is a regime of confinement in which the confinement degradation with power is not as severe as in the L-mode. It has so far been seen only in properly optimized divertor discharges. Thus, the data are not as extensive as for the L-regime and only four different scalings have been proposed. There appears to be a direct correlation between a discharge evolving into an H-mode and the edge electron temperature (or its gradient). In fact, a key feature of the H-mode appears to be the presence of a "hot" edge and a minimization of edge cooling due to neutral recycling and impurity radiation. Except for the power dependence [$f(P) \sim P^0$ below the MHD β limit and $f(P) \sim P^{-(1/3-1/2)}$ near the beta limit] and the magnitude of τ_E which is higher than that observed in L-mode discharges, many of the features of L-mode scaling carry over to the H-mode. The H-mode confinement time is generally 1.5 to 3 times the L-mode confinement time and often is close to the confinement time observed with ohmic heating. The improvement of τ_E (H-mode) over τ_E (L-mode) increases as the edge cooling due to recycling neutrals and impurity radiation is reduced.

3.2 Confinement Projections for CIT

Using the various confinement scalings, projections can be made for the confinement for CIT. These projections have, of course, uncertainties since (1) there are a variety of scaling laws which fit the existing tokamak data but have different projections for CIT parameters, and (2) the impact of alpha heating on confinement is uncertain. In order to have the greatest possible confidence in assuring ignition, the CIT is designed assuming that alpha heating degrades confinement just the same as auxiliary-heating power.

Since the ohmic scalings represent an upper limit to the confinement, we use a combination of the ohmic and auxiliary scalings of the form¹⁹

$$1/\tau_E^2 = (1/\tau_{E,aux}^2) + (1/\tau_{E,OH}^2)$$

to limit τ_E , where $\tau_{E,aux}$ is the auxiliary-heating confinement time and $\tau_{E,OH}$ is the ohmic heating confinement time. For the last four H-mode scalings, we used $\tau_{E,aux}$ (H-mode) = $2\tau_{E,aux}$ (L-mode). Figure 3 graphically illustrates these projections. For the confinement scalings considered, the average confinement times achievable are: $\bar{\tau}_E = 250 \pm 80$ msec for 10-MA L-mode scaling and $\bar{\tau}_E = 400 \pm 75$ msec for 9-MA H-mode scaling.

Ignition depends crucially upon the density profile. Discharges with relatively flat density profiles, which would be expected with gas fueling and strong, short-period sawtooth oscillations, require higher confinement times for ignition than do discharges with the relatively more peaked density profiles, which would be expected with pellet fueled discharges not dominated by large sawtooth oscillations. The reference CIT with flat density profiles easily ignites (using ICRF heating) with the ohmic-heating and H-mode scalings. It also ignites according to many of the L-mode scalings, and $Q > 10$ should be accessible with modest auxiliary power ($P_{aux} \approx 10-15$ MW) even under the more pessimistic L-mode scalings and flat density profiles. This result is illustrated in a typical plasma performance power balance contour plot for representative ohmic-heating (neo-Alcator), H-mode, and L-mode scalings (Fig. 4). The CIT has been provided with a divertor to access H-regime confinement.

It has been observed recently on TFTR and many other experiments, such as PDX,²⁰ Alcator-C,¹⁸ and ASDEX²¹, that very peaked density profiles can be produced with pellet fueling (Fig. 5). This type of peaked profile (compared

to the usual "flat" profiles) greatly reduces the energy confinement time required for ignition in CIT (from ≥ 300 msec to ~ 200 msec). With reasonable peaking ($\alpha \sim 2-2.5$) where $n(r) = n(0) [1 - (r/a)^2]^\alpha$, ignition with L-mode confinement can be achieved (Fig. 6). Indeed, for the somewhat unrealistic highest values of α (~ 4), ignition with ohmic heating appears feasible. For this reason, CIT has provided for a pellet injector which should be able to produce peaked profiles. In addition to improving the central reactivity, there are also experimental indications that such density peaking may improve the total energy confinement. No credit for this latter effect has been taken in our considerations.

4.0 PROJECTIONS OF CIT PLASMA PERFORMANCE

It is useful to have a detailed picture of the projected plasma parameters and performance for the reference CIT cases. Such predictions are helpful in planning the operational scenario and checking its consistency, providing guidance for planning diagnostics, and characterizing the plasma performance for a variety of physics assumptions about confinement, ripple, sawteeth, etc.

The plasma parameters for typical CIT discharge scenarios from start-up to shutdown have been modeled with tokamak transport codes which include detailed treatments of the magnetic geometry, energy and particle transport, and heating mechanisms. The entire discharge scenario has been modeled. Plasma parameters were calculated for both a 9-MA divertor discharge with H-mode confinement and a 10-MA limiter discharge with L-mode confinement. Both of these calculations used relatively flat density profiles. In addition, transport calculations have been done to examine the feasibility of ignition with pellet fueling and peaked density profiles. These calculations have been used to determine the expected plasma parameters, profiles (temperature, density, fusion power, neutron fluxes, etc.), and the time scales for their evolution. The roles of sawtooth oscillations and ripple losses have also been examined. The discharge pulse can be divided into four phases (Fig. 2): start-up, auxiliary heating and ignition, burn, and discharge termination. The performance of each of these phases has been modeled and many of the major issues associated with each phase have been identified and characterized.

4.1 Start-up

The considerations for plasma start-up include: the initial magnetic field configuration, the loop voltage required for discharge initiation, the current ramp-up time, and the poloidal flux consumption. There are sufficient data from existing experiments, and models for interpreting that data, to provide a firm basis for most of the design requirements of the poloidal field (PF) system.

A new factor arises because resistive and nuclear heating of the toroidal field (TF) coils limits the total pulse length in CIT so that the plasma current must be ramped up to its maximum value in the shortest time possible. The design goal for CIT is to reach 10-MA in 3.4 sec. This is faster than has been achieved on existing experiments (3 MA/sec compared to 0.5-1.0 MA/sec). However, this limitation may be overcome by simultaneously bringing the PF and TF systems to full values or by simultaneously increasing the plasma size and elongation as the current is increased. The standard experimental procedure is to initiate the plasma after the TF has reached its flattop value. The plasma current ramp-up rate is then limited by skin current formation, which induces disruptions in the latter stages of the start-up. In CIT a limit of about 1 MA/sec would be required for the last half of the current ramp-up to avoid skin currents in a constant size, constant TF start-up.

Growing the plasma size (vertically or horizontally) can overcome the skin current problem, even at 3 MA/sec ramp-up rates, as demonstrated in the Tokamak Simulation Code (TSC) simulations. The results of two current ramp-up calculations using the Tokamak Simulation Code²³ in which the plasma is grown off the outer and the inner walls are illustrated in Fig. 7. The plasma current increases from 200 kA to 10 MA in 3 sec in the outer wall case and from 500 kA to 9.5 MA in the inner wall case. In each case, this corresponds to a current swing from +6.04 to -5.82 (MAT) in the Pf1 coil and from +13.0 to -11.3 (MAT) in the Pf2 coil, which is the maximum range for these coils. The central density increases from 10^{13} cm⁻³ to 10^{15} cm⁻³ during this period, and the temperature is computed self-consistently. In each case, the plasma current evolves without appreciable skin currents and the q profile remains single-valued. A second technique to achieve the required fast current rise rate is to simultaneously ramp-up the toroidal and poloidal fields (Fig. 2) so that the q profile remains relatively constant during the ramp-up. The

compression aids the penetration of the current so that 3 MA/sec can be reached in either fixed-sized or growing-sized plasmas without attendant skin current problems. This technique has the added advantage of minimizing the resistive heating of the TF coils so that the maximum flat-top pulse can be obtained. Also, initiation at low TF values reduces the fill pressure and breakdown voltage requirements, and TF compression facilitates the density rise and provides modest heating. The use of either or both techniques should allow the current to be ramped up in the required 3.4 sec.

A second aspect of start-up is the requirement that the poloidal field system be able to start and maintain a high- β 10-MA plasma for ~ 3.7 sec. Detailed calculations indicate that the volt-second consumption for a 10-MA plasma during a 3-sec start-up phase consists of about 9.6 ± 0.3 V-sec internal flux, 10.8 ± 0.2 V-sec external flux, and 4.2 ± 0.5 V-sec dissipated by sawtooth activity and neoclassical resistivity with $Z_{\text{eff}} = 1.5$. The uncertainties arise from variations in the current profile, the shape of the plasma boundary, and the plasma resistivity and sawtooth model, respectively. This is a total of 24.6 ± 1 V-sec. The poloidal field system can provide 26.2 V-sec, including contributions from the equilibrium field which are only fully available for the high-beta case. The loop voltage during the 3.7 sec flat-top burn in D-T is 0.3-0.5 V so that the total volt-second requirement for a high-beta 10-MA pulse is 26.1 ± 1.4 V-sec, which is within the 26.2 V-sec capability of the poloidal system. Two additional V-sec would provide an adequate margin for operation of a full length ohmic discharge and cover the uncertainties in the V-sec requirements. They will be added to the design in the next phase.

4.2 Auxiliary Heating and Ignition

Auxiliary heating is required for ignition under the confinement assumptions described in Sec. 3.2. The required auxiliary power has been determined from both steady-state and time-dependent analyses. The results from three reference models are summarized in Table 5; the relationships between these and other confinement projections are discussed in Sec. 3.1. The steady-state auxiliary powers ($P_{\text{aux}}^{\text{SS}}$) listed in Table 5 are required, in each case, to balance losses in the region between the ohmic and ignited states. The net auxiliary power (P_{aux}) is obtained by adding a nominal 5 MW to the steady-state values so that the thermal rise time is reduced to a few

energy confinement times. The neo-Alcator model yields the largest energy confinement time. H-mode confinement is taken as typical of divertor operation and L-mode of limiter operation. Peaking the density with pellet fueling will also reduce the power required for ignition with L-mode scaling. Eight megawatts is required for the most optimistic case and higher powers are required for the more pessimistic scalings. The CIT will operate initially with 10 MW and there are provisions for an additional 10 MW should it prove necessary.

The auxiliary-heating system should be capable of covering the entire TF flattop time of 3.7 sec (or longer if initiated before the end of the TF ramp-up). This condition is dictated by driven plasma operation in H, D, or D-T phases of the experiment.

In all cases sawtooth activity dominates confinement in the plasma core, flattening the current, density, and temperature profiles. Studies have been done using the Kadomtsev reconnection model in transport codes to simulate the effects of the large sawtooth oscillations on CIT. These calculations indicate that (1) due to the effects of elongation and the low q at the edge, the $q = 1$ radius occurs at a $r = 0.5-0.65a$, and the sawtooth mixing region extends over 70% of the plasma half-width, (2) a long sawtooth period is conducive to ignition while a short sawtooth period can prevent ignition, and (3) once the plasma is hot, the shape of the current profile remains essentially fixed (with very little current penetration) on the time scale of a sawtooth period. Even a modest relaxation of the sawtooth effects (i.e., lengthening the period from 100 msec to 200-300 msec, or reducing the impact on ion temperature and density profiles) leads to improvements in central confinement.

The sawtooth mixing region extends over 70% of the plasma half-width at full current partly because of the low safety factor q limiter ($q \approx 2.6$) and partly because magnetic shear is naturally enhanced near the edge of elongated D-shaped plasmas (making q drop more rapidly to unity). If the total current is reduced in these elongated plasmas, the decrease in the breadth of the sawtooth mixing region is slower than linear because the elongation of the inner flux surfaces is reduced with less current, thereby reducing the central current density for a given central q value.

Sawteeth with such a broad mixing region have been observed in the Doublet III²⁴ and PBX experiments under similar conditions of elongation and

large plasma current. In these experiments, L-mode confinement continues to improve with increasing plasma current up to the disruptive limit. Transport simulations using the Kadomtsev reconnection model predict electron temperature mixing in good agreement with experimental electron cyclotron emission (ECE) data.

The effect on ignition of varying the sawtooth period is illustrated in Fig. 8. During the longer sawteeth period, the central ion temperature rises to 38 keV before each sawtooth crash, producing large bursts of alpha heating which keeps the plasma ignited. This central temperature rise is cut off prematurely by the shorter sawteeth, reducing the strength of each alpha heating burst.

Transport calculations (Figs. 9 and 10) indicate that ignition can occur even with L-mode scaling if the density is peaked. Two pellets were injected into the initially cold plasma to peak the density profile. Twenty megawatts of ICRF heating was used at $r = 0.5a$ to delay the current penetration and the onset of sawtooth oscillations. With pellets and 2.0 sec of off-axis heating, ignition was achieved with L-mode scaling (with $\tau_E \sim 200$ msec). With the same L-mode confinement scaling and centrally peaked heating with no pellets, ignition was not achieved (Figs. 9 and 10). In the ignited case, sawtooth oscillations appear a few seconds after ignition because of the strong central peaking of alpha-particle heating and, if the sawtooth period is short enough, may cause loss of ignition.

4.3 Burn

The entire discharge pulse has been modeled and the results of a time-dependent D-T simulation with L-mode confinement and a flat, gas-fueled density profile are shown in Fig. 11. The current and toroidal field have been ramped up from 10% to 100% of the flattop values over a 3 sec start-up phase, while the density ramp-up is stretched out to 4 sec in order to minimize the required auxiliary-heating power and time to ignition. An auxiliary heating power of 20 MW was applied at 2.5 sec (0.5 sec before full-field values are reached to maximize the time in the high temperature burn phase) until the end of the TF flattop at 6.7 sec. It takes about 3.0 sec to reach a nominal thermal steady state. Even though the plasma is subignited, the power balance is dominated by alpha heating with $Q \approx 15$, the central fast-alpha density reaches $\approx 8 \times 10^{18} \text{ m}^{-3}$, and about 30% of the central

pressure is due to fast alphas. These parameters are large enough to allow examination of the thermal, kinetic, and MHD due to effects of the fast alphas. A total of 4.2×10^{20} D-T neutrons are produced, at least as high as any ignited cases examined (which typically are allowed to burn at densities below the nominal limit to help control the burn). Table 6 summarizes classical expectations of the relative fast-alpha density and beta contributions (which are functions only of the local plasma temperature). Due to uncertainties in the scaling of sawtooth oscillations phenomena, the burning properties of an ignited plasma with L-mode confinement and peaked density profiles cannot be easily characterized. If the sawtooth period is long (~0.5-1 sec) or the onset of the sawteeth can be delayed, ignition, or near-ignition, conditions will prevail (Figs. 9 and 10). If the period is short (~0.1 sec), then the plasma will cool to ~5 keV during the current flat-top. The exploration of these phenomena is one of the goals of CIT.

The results of a time-dependent simulation for an H-mode case with 9-MA of plasma current (operation with a poloidal divertor) is shown in Fig. 12. As in the L-mode case, there is a 3 sec toroidal field and current ramp-up time. Due to the lower minimal power requirements compared to the L-mode case, 20 MW of ICRF applied for 1.5 sec is sufficient for ignition. Due to the lower density, most of the characteristics of the plasma are similar to the driven L-mode case except that thermal behavior is entirely governed by alpha heating.

Ripple-induced ion conduction losses are small (with 1.5% peak-to-average ripple at the plasma edge) due to the high plasma density and, therefore, higher collisionality relative to larger tokamak ignition designs (e.g., INTOR) and the rapid fall off of the ripple due to the relatively large number of toroidal field coils. Similarly, in view of the high density and, correspondingly, short thermalization times in CIT, ripple-induced losses of energetic particles, such as alphas and ICRF-heated ions, are not expected to pose a difficulty.

Since an ignited plasma goes through a thermally unstable period, burn control may be important for CIT. The wall loading must be kept within design limits, and it may be necessary to keep beta below a certain value to prevent disruptions. However, if the discharge "runs away," the capability for terminating the pulse exists and will be used to protect the machine. In addition, it is desirable to independently control the plasma temperature and

power level in order to optimize performance. Steady-state burn control is thus an extremely desirable goal. Active feedback through adjusting the fueling mixture (using H pellets, etc.) and impurity control (artificially introducing impurities) may also be feasible burn control techniques for an ignited plasma. There are a number of possible passive burn control mechanisms for an ignited plasma: (1) ripple losses coupled with plasma radial motion, (2) cyclotron radiation dominated power losses in the high field regime, (3) the stabilizing effects of a soft beta limit due to ballooning modes, and (4) operation in a high-Q subignited state with the input power used for thermal control.

4.4 Shutdown

Shutdown can be accomplished by reversing the start-up sequence. In the same manner that TF compression assists current penetration, decompression helps remove the plasma current. In the L- and H-mode time-dependent cases in Figs. 11 and 12, a 2 sec decompression stage was modeled with both current and toroidal field being ramped down linearly in time.

A potential problem is ramping down the plasma density. Depending on the particle absorption rates of the carbon tiles, particle pumping of at least 10% of the charged particle flux may be required to bring the density down over the same 2 sec interval. In ignited plasmas, it may be desirable to begin to reduce the density sometime before the magnetic field ramp-down to de-ignite the plasma, bringing the thermal energy down ahead of the magnetic energy so the beta limit is not exceeded. Good control of the TF and PF systems, as well as the plasma density, will likely be required to avoid disruptions.

5.0 AUXILIARY HEATING

The basic purpose of the CIT auxiliary-heating system is to add the heating power required to increase the temperature of the ohmically heated plasma to the point of ignition. The heating method selected for this purpose is fast-wave ion-cyclotron heating (ICRF), which has demonstrated efficient ion heating at high power and which can be implemented in a high-density tokamak plasma using rf sources currently available at reasonable cost. Other heating methods, such as electron-cyclotron heating, ion Bernstein wave heating, or lower hybrid heating/current drive, are at an earlier stage in

their experimental or technological development and will not be considered in this report. These methods are promising, however, and their progress needs to be monitored for possible future consideration for CIT. In particular, ECRH systems with free electron laser sources may become a backup to ICRF.

The primary issues to be considered in applying ICRF to CIT include: (1) specification of the required rf power, which must be determined self-consistently with the expected effect of the rf heating on confinement, (2) determination of the optimal ion-heating mode, (3) determination of the resonant ion equipartition with the background plasma, and (4) optimization of the launched wave spectrum consistent with the maximum allowable antenna power density. In conjunction with the latter topic, a careful design of the antenna needs to be carried out which maximizes the power handling capability while minimizing the generation of impurities.

5.1 Summary of the Experimental Data

Efficient ion heating at high rf powers has been demonstrated experimentally at both the second harmonic of the majority species (PLT, ASDEX) and at the fundamental cyclotron frequency of a minority ion component (TFR, PLT, JFT-2, ASDEX, TEXTOR). The highest power results reported to date stem from ^3He -minority-heating experiments on PLT¹⁶ as shown in Fig. 13. Associated with this heating is a degradation in the global energy confinement relative to the ohmic values. The initial degradation indicates an L-mode scaling, but shows a saturation at high power. However, the range of data is somewhat limited. Results from other minority heating experiments show similar confinement degradations, although one (ASDEX) indicates that improved confinement (H-mode) is possible with a combination of ICRF, neutral-beam heating, and a divertor. Second harmonic majority heating has also been demonstrated at slightly lower heating efficiencies. In ASDEX experiments, it was found that the injection of fast particles via neutral beams served to improve the heating efficiency of this rf mode. In PLT it was observed that, at sufficiently low minority H concentrations, second harmonic resonant deuterium could be made to absorb a significant fraction of the wave power, resulting in direct majority heating. In all of these experiments, no fundamental limit to wave penetration was observed up to the highest densities investigated ($n_{e0} = 2 \times 10^{14} \text{ cm}^{-3}$).

In these experiments an increase in both low-Z and high-Z impurities is observed roughly proportional to the rf power. Although no direct link has been conclusively demonstrated, the experimental data (PLT, ASDEX) indicates that the loss of rf-induced fast ions may be responsible for the generation of impurities by sputtering. Proper choice of the limiter and antenna materials has been shown to limit the resulting impurity radiation losses to low-Z edge radiation (PLT, ASDEX, TFR). Under properly optimized conditions, the central energy confinement in these experiments was unaffected by impurity radiation losses, although some edge cooling may have prevented the achievement of H-mode confinement with ICRF alone in ASDEX.

5.2 ICRF Heating Strategy for CIT

Based on these experimental results, either second harmonic majority or fundamental minority heating are considered to be viable for CIT. Although the scaling laws for energy confinement are somewhat uncertain, the maximum power required is taken to be 20 MW, which is to be provided by an array of antennas. A variety of heating modes are accessible with a single rf source and antenna configuration by choosing the resonant ion species, operating toroidal field, and wave frequency as shown in Table 7. Due to the efficiency of minority heating in even a low-beta start-up plasma and the availability of rf power sources, the primary heating scheme for CIT has been chosen to be ^3He -2T at 90 MHz for a design field of 10 T. Fixed frequency operation would permit H-minority heating at 6 T, while source tunability to 135 MHz would permit full-field experiments in this mode as well. While variable frequency sources are not required to cover the expected operating range, some tunability may be desirable from an operational point of view. The viability of such an option depends largely on the cost impact on the rf power sources and matching systems rather than on physics requirements. The advantage of ^3He -minority heating derives in part from the fact that strong single pass absorption is expected even during the start-up phase and it could be replaced by second harmonic tritium heating as ignition conditions are approached (Fig. 14). Moreover, in this mode the competition for wave absorption from the alphas is minimized. Other considerations influencing this choice include an expected enhancement of the achievable power per port at the comparatively lower ^3He resonance frequency and the existence of readily available power sources.

The absorption calculations shown in Fig. 14 indicate that the antenna k_{\parallel} selection is not critical but is optimal in the range $0.05-0.15 \text{ cm}^{-1}$. The transition between ^3He and T heating occurs around 1% ^3He concentration. Similar results are found for the D-H case. Power deposition calculations indicate that strong wave focusing is feasible, resulting in a focal spot considerably smaller than the expected $q = 1$ surface. In accord with present experimental results, it is assumed that sawtooth oscillations (or other unspecified causes) broaden the rf power deposition profiles to a volume corresponding to the sawtooth inversion radius. Under these circumstances the central rf power density is too low to produce appreciable ion-tail generation at CIT operating densities. The resonant ions are strongly coupled to the bulk ions producing primarily ion heating within the $q = 1$ surface. (An exception can be found in the case of vanishingly small ^3He concentration whereby, ion-tail "temperatures" in the range of 100-200 keV can be produced resulting in some central electron heating.) No enhanced fast-particle losses are expected with the large plasma currents for CIT. In addition, the absence of fast-ion tails may result in the avoidance of appreciable impurity generation.

The major uncertainties of this heating method are associated with the effect of auxiliary heating on confinement itself, i.e., the extent to which L-mode scaling will govern energy confinement. Related to this issue is the question of whether or not wave focusing will function according to the theoretical model in depositing the rf power in a region considerably smaller than the $q = 1$ surface.

5.3 Antenna Physics

Once the frequency and total power requirement have been chosen, the optimal antenna design requires a trade-off of the conflicting requirements to maximize coupling (antenna close enough to the plasma so that there is some plasma near the antenna) and to minimize the damage to the antenna and impurity generation (antenna far enough from the plasma to prevent erosion and impurity generation due to the heat flux from the plasma). An antenna array based on currently existing inductive loop technology appears to be workable in the CIT design, provided the loops are adequately protected in recesses in the vacuum vessel wall. The radiated efflux is expected to be about 60 W/cm^2 during a full power burn. In a four-second-burn pulse this will cause a

significant but manageable temperature increase of the antenna components in the line-of-sight of the plasma. The power flowing along and diffusing across field lines would give a maximum heat load to one antenna of about 70 kW/cm². Fortunately, most of this power appears on the divertor plates or limiters. If necessary, however, secondary limiters can be located near the antennas to keep streaming losses to the antennas at a tolerable level. A Faraday shield is required to force the polarization of the launched waves to be primarily in the fast wave and to protect the radiating elements from plasma contact. Antenna loading estimates indicate 2-5 ohms radiation resistance, which is marginally adequate to handle 3-4 MW per port. These estimates, in turn, depend critically on the edge density and the scrape-off thickness. If the antenna Q is estimated to be about 20, then a commonly used maximum voltage limit of 60 kV permits approximately 3.5 MW per port. The average power density is about 2 kW/cm², which is slightly larger than that obtained in present experiments.

6.0 MAGNETICS

The major magnetics questions for CIT include the design of the poloidal field system, the vertical stability and control of a high-beta, low-q, highly elongated plasma, and the beta limit.

6.1 Axisymmetric Magnetics

The Princeton Tokamak Simulation Code (TSC)²³ has been applied to the design of CIT to study current ramp-up, vertical control, and shape control. This code has recently been validated by incorporating the Coppi/Tang transport model and by performing detailed comparisons with PBX and TFTR data. The results of these comparisons are that the simulation code is accurate enough to reproduce the plasma position to within a few centimeters, and the loop voltage to within 10%, even during transient periods, such as current ramp-up when the external fields are changing rapidly and the eddy currents in the conductors are substantial.

Without any passive stabilizing conductors, the 10-MA plasma will be unstable to a nearly rigid vertical axisymmetric instability with a growth time of 0.6 μ sec. Perfectly conducting plates will stabilize this, provided they are close enough to the plasma. The critical separation distance from the plasma for two horizontal plates is $\Delta Z = 25$ cm. Vertical plates with an

inside separation of 10 cm and an outside separation of 22.5 cm will also stabilize this mode.

The 15-mm-thick tight-fitting stainless steel vacuum vessel shown in Fig. 15 is clearly adequate to provide stability on the ideal MHD time scale. The vessel is resistive, however, with a L/R decay time of 5 msec. Calculations show that this vessel will slow the unstable mode to a growth time of 16.7 msec.

Active feedback control coils located at $R = 1.32$ m, $Z = \pm 1.00$ m are sufficient to completely stabilize the mode. A current of ± 150 kA in each of these coils is sufficient to hold the plasma 5 cm off the midplane. To return the plasma to the midplane in one 16.7 msec growth time should require a peak power of no more than approximately 50 MW on a transient basis.

The option of adding aluminum stabilizing plates just outside the vacuum vessel but inside the TF coils (Fig. 15) has been also considered. These plates will slow the unstable mode to a growth time of 350 msec reducing by a factor of 20 the real power required to return the plasma to the midplane in one growth time.

6.2 Beta Limits

The Troyon-Gruber¹⁰ criterion has been chosen as a constraint in the CIT design:

$$\beta(\%) = C_T I(\text{MA}) / [a(\text{m}) B_T(\text{T})].$$

Experimental data suggest that a value of C_T in the range of 3.0 to 3.5 is routinely achievable for a broad range of tokamak discharges. Theoretical studies have shown that C_T is somewhat dependent upon shape and plasma profiles, but optimization studies for reasonable shapes and current distribution lead to about the same value as that observed experimentally.

In addition to application of the general guideline, several detailed studies have been carried out for the CIT and similar configurations. A key result of these studies has been that the present triangularity, $\delta = 0.2$, is sufficient to attain the desired value of $C_T = 3$ with the elongation ($\kappa = 1.8$) chosen for CIT. To assure that there is a range of acceptable operation and to provide data for system trade-off studies, κ values of 1.6 to 2.5, δ values of 0.3 to 0.4, and limiter q values of 2.6 to 3.1 have also been analyzed with

$q_0 = 1$, as have cases with and without a field null (poloidal divertor) at the edge of the plasma. (An aspect ratio $A = 3$ was used for many of these studies, which were carried out for a previous version of CIT, leading to beta limits slightly lower than would be the case for the present design, which gains slightly in beta from the reduction of A to 2.7). With internal mode optimized pressure profiles which tend to be broad and safety factor profiles of the form $q(\psi) = 1 + (q_e - q_0) \Psi^\alpha$ (where Ψ is the unity normalized poloidal flux function), ballooning modes are stable even for some values of C_T greater than 3 for the above parameter space. For these profiles, unstable low-mode-number external kink modes result under the pessimistic assumption of no conducting wall stabilization. Stability is obtained when a wall is closer than 0.25 minor radii from the plasma edge. The conducting structure of CIT will lie closer to the plasma than this. The design value of $\beta = 6.3\%$ then appears, from the point of view of ideal MHD studies, to be aggressive but reasonably safe if nature and profile control measures yield the appropriately broad profiles. As is shown below, additional edge shear can be used to stabilize the external kink mode while preserving $C_T > 3.0$.

Sawtooth oscillations in tokamaks are believed to cause broad profiles with the flattened regions near the center and the gradients concentrated near the outer regions of the discharge. The Doublet-III device has been operated in the presence of such sawteeth to a beta value corresponding to C_T of just over 3.25.²⁴ A modeling study has been carried out using the 1-1/2 dimensional BALDUR transport code with a semiempirical sawtooth model and the PEST stability analysis package. The flat q profiles inside the sawtooth inversion radius with steep edge shear stabilize the external kink modes, even without wall stabilization. However, pressure peaking on axis due to alpha-particle heating can lead to internal mode instability inside the inversion radius. Transport models which take account of this by flattening the pressure profile inside $q = 1$ are being developed. Preliminary results for near-ignited scenarios that are internal and external mode stable with no structure have already been obtained. The addition of pellet fueling into the transport model should lead to stable ignition. As indicated before, the Doublet-III experience suggests that stable $C_T = 3$ discharges can be obtained even with large sawteeth.

6.3 Fishbone Instabilities

Alpha-particle confinement is essential for ignition. "Fishbone" oscillations have significantly degraded the effectiveness of neutral-beam heating for a number of tokamaks by causing loss of the neutral-beam fast ions.²⁵ We have considered possible alpha-particle-induced fishbone instabilities for the CIT device. The alpha-particle trapped fraction and precession rate were obtained by Monte-Carlo simulations using isotropic pitch angle distributions in PEST generated equilibria. The critical trapped particle $\beta_{\alpha, \text{crit}}$ for fishbone destabilization is given by

$$\beta_{\alpha, \text{crit}} = \frac{1}{4} \frac{\langle \omega_d \rangle}{\omega_A},$$

where ω_A is the Alfvén frequency and $\langle \omega_d \rangle$ is the distribution-averaged precession frequency. The expected alpha-particle β_{α} during an ignition experiment depends on scaling assumptions. Ohmic (neo-Alcator) scaling gives $\beta_{\alpha} \approx 1\%$ and Kaye-Goldston L-mode scaling gives $\beta_{\alpha} \approx 0.3\%$. For ohmic scaling, the trapped particle $\beta_{\alpha}/\beta_{\alpha, \text{crit}}$ is 7.5 for CIT, indicating a high probability of alpha-particle induced fishbones. Steady fishbone bursting would limit the trapped alpha-particle β_{α} on average to the threshold value β_{crit} , thereby causing an approximate 25% reduction in the total (trapped and passing) alpha-particle population. With L-mode scaling, fishbone bursting is less likely. With H-mode scalings, the alpha-particle losses should also not be large enough to affect ignition. The absence of strong ICRF tails at CIT densities implies that ICRF-induced fishboning will not be important.

7.0 IMPURITY AND PARTICLE CONTROL

The major impurity control issues for CIT involve determining the peak heat loads for the limiters and divertor plates and assessing the performance of the CIT poloidal divertor. The major particle control issue is the effectiveness of fueling with pellet injection.

7.1 Plasma Edge Characteristics

The edge characteristics of CIT are important in determining the in-vessel component heat fluxes as well as the radial position of rf wave-launching structures (transmission through the edge plasma). Extrapolation of present-day experiments to CIT has been made using a combination of results

from high-density tokamaks (Alcator-A, Alcator-C, FT) with mechanical limiters and low-density tokamaks (ASDEX, D-III, PDX) with divertors. Using the most complete set of such data available, the density e-folding length (λ_n) from a number of tokamaks is proportional to $(L/B)^{1/2}$ (Fig. 16), where L is half the connection length along a field between material surfaces, and B is the toroidal magnetic field. The justification for such a plot comes from the simple relation:

$$\lambda_n = \left(\frac{LD}{v_{\text{sound}}} \right)^{1/2},$$

where the radial diffusion coefficient D is assumed to be Bohm-like, and V is the ion sound space. On the basis of a linear fit to this data, the λ_n for CIT is ≈ 1 cm. Due to the tendency of the electron temperature e-folding length to be larger than λ_n , the e-folding length for power flow in the CIT edge plasma is expected to be ≈ 0.5 cm. This result was also obtained by directly scaling λ_n from Alcator-C results.

In a similar fashion, approximate values of electron density and temperature at $r = a$ can be derived. At the highest operating densities of Alcator-C ($\bar{n}_e \geq 4 \times 10^{14} \text{ cm}^{-3}$), $n_e(a) \approx 0.5 \bar{n}_e$, therefore, an upper bound on $n_e(a)$ for CIT can be estimated to be $\leq 2.5 \times 10^{14} \text{ cm}^{-3}$. $T_e(r = a)$ has been calculated from the above information and simple scaling rules from sheath theory. Over the range in input power flowing into the edge plasma, 2-40 MW, the edge temperature would vary from 28 to 65 eV. These estimates are in rough agreement with the more detailed calculations described in the next section, although, of course, the divertor changes these values somewhat.

7.2 Divertor Operation

There are two driving forces which mandate inclusion of a poloidal divertor in CIT: (1) the ability to access H-mode confinement and (2) minimization of the impurity level in the plasma. The CIT divertor design is shown in Fig. 17.

The divertor configurations of present and past devices (ASDEX, PDX, D-III) have enabled H-mode confinement to be achieved with the concurrent application of sufficient neutral-beam heating.¹³ On the basis of those results, the principal criteria for achieving H-mode confinement appear to be that an X-point be within the vessel and that the plasma edge just inside the

separatrix be "hot," which requires that the neutral density and impurity radiation at the plasma edge be low. The physical criteria used in the CIT divertor design corresponding to the above requirements are that: (1) the recycling be localized away from closed flux surfaces (i.e., at a divertor plate), (2) that the distance between the last closed flux surface and any material objects in the vessel be $\geq 1-2 \times \lambda_n$, the density scrape-off length, and (3) that the distance from the separatrix/divertor plate intersection to the X-point be $\approx 3-5 \times \lambda_{mfp}$ (ionization and charge-exchange) for recycling neutrals. The first two criteria are clearly fulfilled by the divertor geometry shown in Fig. 17. This geometry was chosen to provide a uniform heat flux on the divertor plate and to localize the neutral recycling. Estimates of the mean-free-paths for ionization and charge-exchange of H^0 were used to evaluate the third criteria. These vary from ≈ 4 cm at $n_e \sim 10^{14} \text{ cm}^{-3}$ to 0.3 cm at $n_e \sim 10^{15} \text{ cm}^{-3}$. The operating point envisaged for the ignited CIT as detailed in the modeling is in the range of $n_{e,plate} = 0.4-1.2 \times 10^{15} \text{ cm}^{-3}$. The mean-free-paths for neutral deuterium or tritium (which are smaller than H^0 by $\sqrt{2}$ and $\sqrt{3}$, respectively) should be much smaller than the distance from the X-point to the divertor plate (≈ 15 cm). Under the assumption that the above criteria apply equally well to a high-density diverted tokamak with ICRF heating and to neutral-beam heating on low-density diverted experiments, the CIT should be able to access the H-mode confinement regime.

The whole of the CIT scrape-off was modeled by means of 2-D plasma and neutral transport codes (Fig. 17). The purpose of modeling was to estimate the general scrape-off plasma properties and to make sure that the recycling region stays outside the separatrix.

The detailed model examines steady-state equations for solutions determined by boundary conditions. One of these conditions is the particle flux from the main plasma across the separatrix, which was set to zero for the present calculation because pumping has not been provided. Instead, the total neutral flux was imposed from the plates, such as to give the desired plate temperature and the expected density on the separatrix (midplane) of $\approx 2 \times 10^{14} \text{ cm}^{-3}$. In addition to this neutral flux, which was set at 5.2×10^{24} atoms/sec, a power of 24 MW into the outer and 18 MW into the inner scrape-off was assumed. These input parameters result in a peak plasma temperature of 35 eV and a peak plasma density of $1.5 \times 10^{15} \text{ cm}^{-3}$, at the plate. The plasma density along most of the plate, however, was only $\approx 4 \times 10^{14} \text{ cm}^{-3}$. The

midplane-separatrix values are $n_e = 2.2 \times 10^{14} \text{ cm}^{-3}$ and $T_e = 90 \text{ eV}$. There is a substantial gradient in the density and temperature along the field lines. The temperature T_e drops from 90 eV at the midplane to 30 eV at the plate. The plasma densities at the plate, $2 \times 10^{14} - 15 \times 10^{14} \text{ cm}^{-3}$, are high enough to confine the neutrals to a region close to the plate and away from the main plasma (Fig. 18).

The radial power flow in the scrape-off is a function of the thermal diffusivity, which was taken to be $\chi_{\text{total}} = 4 \times 10^{11} \text{ cm}^2/\text{sec}$. As mentioned in Sec. 7.1, the e-folding length for power flow was estimated from experiments to be $\lambda_{\text{power}} \approx 0.5 \text{ cm}$. To compare with this estimate, we mapped our computed plate power densities onto the midplane and found $\lambda_{\text{power}} \sim 0.75 \text{ cm}$. The two estimates are in reasonable agreement in view of the uncertainties. Thus, the optimized shape for the plate can be determined reasonably accurately by a simple mapping of an exponential midplane power profile onto the plate.

The attainment of a clean (low-impurity density) plasma is a byproduct of a divertor optimized to achieve H-mode confinement. The mean-free-path for ionization of any neutral impurity is significantly shorter than for a hydrogen atom. In addition, as indicated by the high electron density at the neutralizer plate and the gradient in T_e along a field line, the divertor is operating in a high-recycling state. This lowers the ion-impact energy and resultant sputtered fluxes. This "high-recycling" regime has the additional advantage of reduced charged-particle heat flux at the neutralizer plate due to radiation in the scrape-off layer and the region near the plate. The calculated edge plasma conditions are listed in Table 8.

7.3 Limiter Operation

The CIT is designed to operate with a strictly mechanical limiter configuration as well as with the divertor described above. The inner bumper limiter is designed to accept the full heat loads (shown in the engineering section) envisaged for CIT.

7.4 Density Control and Fueling

Fueling is needed during the initial density rise and during the flat-top period, both to maintain the density and to provide density profile control. Adequate gas puffing should be provided to establish and maintain the specified density of $6 \times 10^{14} \text{ cm}^{-3}$ (about 6×10^{21} atoms or 100 Torr-liters of

H₂). During ramp-up, the fueling rate has to be at least 35 Torr-liter/sec and should be somewhat larger (50 Torr-liter/sec) to allow for some recycling losses (based on Alcator-C and TFTR experience). Maintenance of the density during the discharge should be possible with this system as well.

Pellet fueling is highly desirable. The presence of carbon tiles in Alcator-C limits the maximum density $\langle n \rangle$ to about $3 \times 10^{20} \text{ m}^{-3}$ with gas puffing. Pellet fueling not only allows this limit to be exceeded substantially, but allows some control of the density profile as well. Figure 19 shows a calculation of the relative penetration into the plasma of pellets which would provide a Δn of $\sim 10^{20} \text{ m}^{-3}$, which indicates that a pellet speed of $\sim 2 \text{ km/sec}$ would be adequate. There are some experimental indications that these calculations may underestimate the pellet penetration, and that the actual penetration may be better for CIT. The pellet injector specification was set to allow the injector to do almost all of the initial fueling and to provide up to 5 pellets/sec during the plasma build-up and the flattop. The requirements for both the fueling and pumping are summarized in Table 9. Higher velocity pellets would, of course, be extremely useful, but require very significant development.

7.5 Disruptions

A characterization of disruptions is necessary for assessing the peak power and energy loads on the first wall. The CIT has been designed to handle the forces from a disruption on every shot, so that mechanical loads are not a problem. A design point CIT discharge contains 36 MJ of plasma thermal energy ($1.5 \text{ k} \int \langle n_j T_j \rangle V = 1.5 \text{ } \mu\text{B}_0^2 V / 2\mu_0$), and 104 MJ (0.5 LI^2) of stored poloidal magnetic field energy that must be transferred to the first wall, structure, and coil systems during a major disruption.

The critical CIT disruption parameters and their assumed values (Fig. 20) are:

- Current decay time (10-100 msec based on a maximum rate of 1 MA msec^{-1}),
- thermal quench time (2-10 times faster than current quench),
- fraction of magnetic energy inductively coupled to structure and coil systems (60%),
- fraction of resultant plasma thermal energy radiated (70%),
- fraction of thermal convective/conductive losses deposited

on the limiter/divertor (50%), and

- localization (ratio of peak-to-average) of thermal losses is 2 for the limiter, 1.5 for the divertor.

Figure 20 shows a peak first wall energy flux of 333 J cm^{-2} on the inboard tiles and a divertor flux of 625 J cm^{-2} . The number of full power CIT shots is limited (3000). No lifetime estimates are currently available, although studies are in progress. Based on a 1-msec thermal quench time, the transient power levels of 4 GW m^{-2} to the divertor may lead to substantial ablation of the first wall tiles. We conclude that the peak heat fluxes from major disruptions may lead to relatively short lifetimes for some of the first wall tiles. However, the uncertainties of energy deposition and time scales mean that no firm conclusion can be drawn at this time, and further analysis and experiments are needed. The tiles are designed so that they can be easily replaced, and a remote handling system capable of replacing injured tiles without a vacuum opening is part of the CIT design.

8.0 DIAGNOSTICS AND OPERATIONS

8.1 Operations

The proposed operations plan is outlined in Fig. 21. The strategy of the plan during the first two years is to reach D-T operation as soon as possible and, at the same time, thoroughly check out the machine and physics while using only a minimum of the allowed 3,000 full-field pulses. Operation is scheduled to begin in December 1992.

The initial six to eight months of operation will be devoted to ohmic-heating studies, during which time the machine will be commissioned and checked out. Initial engineering tests will also be conducted for the ICRF system. Some of the physics relevant to the machine will be studied. Following this will be a short fuel field test period to check out the machine performance and to study the physics of ohmic heating. This period will be followed by roughly a year of D and D-He³ studies at reduced field to check out both the machine and ICRF engineering and physics performance. An important part of this check-out period will be the testing of all the diagnostic systems. In early 1995 D-T studies will begin. At first, these studies will be at reduced fields to test out the tritium systems and the remote handling, and to conduct single particle-alpha physics studies. These

studies will be followed by a limited series of full-field shots to map out the physics issues of ignition. Then, about six more months of operation will be devoted to the study of ignition physics. This will be followed by one to three years of studies of burning plasmas.

8.2 Diagnostics

The diagnostic instrumentation on CIT must provide the measurement capability of present-day tokamaks with the added capability of following the alpha physics during the burn phase. The range of physical parameters will be as high as $T_e(0) \sim 30$ keV, $T_i(0) \sim 40$ keV, and $n_e(0) \sim 1 \times 10^{21} \text{ m}^{-3}$. The measurements have to be made with very restricted access to the tokamak and in the presence of a very high radiation background. This background is sufficiently high that shielding of radiation must be an integral part of any diagnostic design to prevent component damage and intolerable noise levels. It also leads to requirements for remote handling, module replacement, mechanical support and alignment, and calibration which are significantly beyond those required at TFTR. A list of the planned diagnostics is given in Table 10.

In addition to these diagnostics, there is interest in diagnostics for measuring the fast-alpha population. A number of techniques have been proposed.²⁶ These include:

- (1) single charge exchange with a fast H beam,
- (2) double charge exchange with a fast Li^0 beam,
- (3) small angle laser scattering,
- (4) lower hybrid damping on alphas,
- (5) detection of fusion gammas, and
- (6) measurement of the ion cyclotron emission.

One or more of these techniques will need to be developed for CIT.

9.0 SUMMARY

The CIT is an experiment designed to explore the physics of ignition with alpha-particle heating at minimum cost. The key physics issues have been discussed in the previous sections. The design parameters described here will change somewhat as further design studies are carried out and the design is optimized. Among the major deficiencies in the current design that are being addressed are the high currents required in the poloidal field system to form

a divertor and high peak heat loads on the divertor plates and limiter.

ACKNOWLEDGMENTS

The authors are grateful to the many groups who contributed to the engineering and physics of the design of CIT. Among these is Professor Bruno Coppi who has pointed out and demonstrated that such a device is both technically feasible and could allow us to address the ignition physics issues with a relatively inexpensive compact experiment. The members of MFAC Panel XIV, chaired by D. Meade, helped develop a set of goals for the experiment. The members of the Ignition Physics Study Group, chaired by J. Sheffield, gave us guidance from the general tokamak community. The members of the Ignition Technical Oversight Committee formulated the physics and engineering guidelines for the experiment. We also gratefully acknowledge the contributions of the CIT engineering teams in the design physics considerations. We are especially grateful to Ms. E. Carey for careful preparation of the manuscript through ten or more versions.

This work was supported by the U.S. Department of Energy Contract No. DE-AC02-76-CHO-3073.

REFERENCES

- ¹STODIEK, W., Nucl. Fusion 25 (1985) 1161.
- ²KADOMTSEV, B. and POGUTSE, O., Reviews of Plasma Physics (Consultants Bureau, Plenum, NY, 1970) pp. 395-398.
- ³COPPI, B., Comments on Plasma Physics and Controlled Fusion 3 (1977) 47.
- ⁴COHN, D.R., WILLIAMS, J., BROMBERG, L., KREISCHER, K., MONTGOMERY, D.B., and PARKER, R.R., in Fusion Reactor Design Concepts (Proc. Tech. Com. and Workshop, Madison, WI, 1977) IAEA, Vienna (1978) 113.
- ⁵JASSBY, D.L., FURTH, H.P., REARDON, P.J., COHN, D.J., and WILLIAMS, J., in Fusion Reactor Design Concepts (Proc. Tech. Com. and Workshop, Madison, WI, 1977), IAEA, Vienna (1978) 67.
- ⁶POST, D., Applied Atomic Collision Physics, Eds. Harison, Barnett (Academic Press, 1984) p. 381.
- ⁷MC ALEES, D., Oak Ridge National Laboratory Report No. ORNL-TM-4661 (1974) 131 pp.
- ⁸KOLESNICHENKO, YA. I., Nucl. Fusion 20 (1980) 727.
- ⁹MILORA, S.L., et al., Nucl. Fusion 20 (1980) 1491.
- ¹⁰TROYON, F. and GRUBER, R., Phys. Lett. 11A (1985) 29.
- ¹¹KAYE, S.M., Phys. of Fluids 28 (1985) 2327.
- ¹²INTOR, International Tokamak Reactor, Phase Two A, Part II, IAEA, Vienna, 1986.
- ¹³WAGNER, F., et al., Phys. Rev. Lett. 49 (1982) 1408.
- ¹⁴UCKAN, N. and SHEFFIELD, J., Oak Ridge National Laboratory Report No. ORNL-TM-9722 (1985).
- ¹⁵MURAKAMI, M., et al., Nucl. Fusion 16 (1976) 347.
- ¹⁶MAZZUCATO, E., et al., in Plasma Physics and Controlled Nuclear Fusion Research (IAEA, Vienna, 1985) Vol. I, 433.
- ¹⁷BLACKWELL, D., et al., in Plasma Physics and Controlled Nuclear Fusion Research (IAEA, Vienna, 1983) Vol. II, 27.
- ¹⁸PARKER, R., et al., Nucl. Fusion 25 (1985) 1127.
- ¹⁹GOLDSTON, R., Plasma Physics 26 (1984) 87.
- ²⁰FONCK, R., et al., J. Nucl. Mater. 128&129 (1984) 330.
- ²¹NIEDERMEYER, H., et al., to be published in proceedings of the European Physical Society (EPS) Meeting (1986).
- ²²BELL, M. and SCHMIDT, G., private communication (1986).
- ²³JARDIN, S., et al., Princeton Plasma Physics Laboratory Report No. PPPL-2258 (1985) 47 pp; to appear in J. Comput. Phys., 1986.

²⁴PFEIFFER, W., et al., Nucl. Fusion 25 (1985) 655.

²⁵WHITE, R., et al., Phys. Fluids 26 (1983) 2958.

²⁶SCHUMACHER, U., this volume.

TABLE 1

Progress in Tokamak Plasma Parameters

	1986	Parameters for the ST tokamak (1970) ¹
Confinement times	0.2-0.4 sec with auxiliary heating (TFTR, JET)	---
	0.4-0.8 sec with ohmic heating (TFTR, JET)	0.01 sec
Beta	4.5-5.0% (D-III, PBX)	0.2%
$T_e(0)$	5-7 keV (JET, D-III, TFTR)	1.5 keV
$T_i(0)$	20 keV (TFTR)	0.4 keV
$n(0) \tau_E$	1.5×10^{20} sec m^{-3} (TFTR)	10^{18} sec- m^3
Heating power	17 MW neutral beams (TFTR) [Prichard, B., 1986]	---
	5.5 MW ICRF (JET)	1 MW ICRF
Impurity control	$Z_{eff} < 2$ (for almost all tokamaks)	$Z_{eff} \sim 5-7$

TABLE 2

CIT Parameters

Major radius (m)	1.22
Minor radius (m)	0.45
Aspect ratio	2.7
Elongation	1.8
Toroidal field (T)	10.4
Plasma current (MA)	10
Pulse length (sec)	3.7
Peak fusion power (MW)	450
Average design fusion power (MW)	300
Peak neutron wall load (MWm^{-2})	11
Average design wall load (MWm^{-2})	8

TABLE 3

Physics Guidelines and Operational Limits

Confinement	adequate margin for ignition with auxiliary heating
"Figure of Merit"	$aB_T^2/q_{cyl} \geq 25$
Density limit	$\langle n_e \rangle < 1.5 \times 10^{20} \text{ m}^{-3} B(T)/[R(m)q_{cyl}]$ (Murakami Limit) ¹⁵
Beta	$\beta (\%) < 3.0 I(\text{MA})/a(\text{m}) B(T)$ (Troyon Limit) ¹⁰
Elongation	$b/a \leq 1.8$
Aspect ratio	$R/a \geq 2.7$
Plasma current	$q_{edge} > 2.6$ $r_{edge} - r_{q=2} > 5 \text{ cm}$ $\geq 10 \text{ MA}$ (with limiter), $\geq 9 \text{ MA}$ (with divertor)
Burn pulse	$\geq 10 \tau_E$
TF flattop pulse	$\geq 12 \tau_E$
Auxiliary heating	10 MW ICRF initially 20 MW ICRF if required
Impurity control	$Z_{eff} \leq 1.5$ limiter plus double null poloidal divertor
Fueling	pellet and gas fueling

TABLE 4

Physics Parameters

Volume-averaged density	$\leq 6.5 \times 10^{20} \text{ m}^{-3}$
Typical operating temperature	10 keV
Critical beta	6.3% (10 MA), 5.7% (9 MA)
Q_{ψ}	2.6
Q_{cyl}	2.0 (10 MA), 2.2 (9 MA)
Current	10.0 MA (limiter), 9 MA (divertor)
Minimum τ_E for ignition	200-350 msec (depends upon profile)
Elongation	1.8 (limiter determined at 96% flux surface)
	1.9 (divertor, determined at the 96% flux surface)
Triangularity	0.2 (limiter determined at 96% flux surface)
	0.4 (divertor determined at the 96% flux surface)
Radial scrape-off decay length	
Density	1 cm
Power	0.5-0.75 cm
Fusion power	300 MW
Alpha heating power	60 MW
Power radiated	18 MW
Power on divertor plates/limiter	42 MW

TABLE 5

Auxiliary Power Requirements

Model	τ_E (sec)	P_{aux}^{SS} (MW)	P_{aux} (MW)	Comments
Neo-Alcator	0.60	3	8	α -heating \approx ohmic heating
Kaye-Goldston H-mode	0.45	5-10	10-15	divertor, α -heating=auxiliary
Kaye-Goldston L-mode	0.30	15	20	limiter, α -heating=auxiliary

TABLE 6

Fast Alpha-Particle Density and Beta Fractions

$T_{e,1}$ (keV)	n_{α}/n_e (%)	$\beta_{\alpha}/\beta_{th}$ (%)
10	0.1	4
20	0.8	19
30	1.8	31

TABLE 7

Frequency Regime:

LOW-FIELD OPERATION: ~6 TD-H, ^4He - H, H minority

- low radiation possible
- low-beta start-up
- possible electron heating

HIGH-FIELD OPERATION: ~10 TD- ^3He , ^4He - ^3He ; ^3He minority

- low-beta start-up
- low radiation possible
- nonresonant alphas

D-T, T second harmonic

- reactive mode
 - nonresonant alphas
-

TABLE 8

Plasma Scrape-off Characteristics

Power entering the edge	42 MW
Power to outer plates	28 MW
Power to inner plates	14 MW
λ_{power} (midplane-separatrix)	1.0 cm
n_e (midplane-separatrix)	$0.75 \times 10^{14} \text{ cm}^{-3}$
T_e (midplane-separatrix)	90 eV
n_e (divertor plate-separatrix)	$\sim 0.4\text{-}1 \times 10^{15} \text{ cm}^{-3}$
T_e (divertor plate-separatrix)	30 eV
P_{avg} on limiter/divertor surfaces	4-6 MW/m ²
λ_{mfp} (ionization of 30 eV D ⁰ at plate)	$\approx 0.2 \text{ cm}$
λ_{mfp} (ionization of 30 eV C at plate)	$\approx 0.05 \text{ cm}$
Distance from x-point to plate	$\approx 15 \text{ cm}$

TABLE 9

Fueling and Pumping Requirements

	Normal Operation	Maximum Requirement
<u>Gas puffing</u>	25-50 Torr μ /sec	500 Torr μ /sec
<u>Pellet fueling</u>		
Velocity	1-2 km/sec	2 km/sec
Pellet radius	1.5-2 mm	2 mm
Composition	H ₂ , D ₂ , T ₂	H ₂ , D ₂ , T ₂
Frequency	1-4/sec	10/sec
Total number	10	40
<u>Pumping</u>		
Between shots	200-500 μ /sec	1000 μ /sec
During discharge cleaning	500-1000 μ /sec	>1000 μ /sec

TABLE 10

CIT Diagnostics

MEASUREMENT	DIAGNOSTICS
Electron density profile	Multipoint Thomson Scattering Infrared Interferometer
Electron temperature profile	Multipoint Thomson Scattering Michelson ECE (and/or Grating Polychromator ECE)
Current density profile	Infrared Faraday Rotation
Ion temperature profile	Charge-Exchange Recombination Spectroscopy Multichannel Neutron Flux Detectors High Energy Resolution Neutron Spectroscopy, Single-point X-ray Crystal Spectrometer
Impurity concentration and radiated power	Visible Bremsstrahlung Interference Filter Array Vacuum UV and X-ray Spectroscopy Bolometers
Magnetic properties	Rogowski Loops Voltage Loops/Saddle Coils Magnetic Coils and Mirnov Loops Diamagnetic Measurement
Wave activity	Mirnov Loops FIR Grating Polychromator Fast Neutron Detectors Millimeter-Wave Scattering
Alpha particles	Escaping Alphas Slow Confined Alphas
Plasma/edge wall	Plasma TV/IR TV Divertor Probes, etc. Visible Filter Scopes
ICRF monitoring	Power Monitor 16 MeV Gamma Spectrometer
Miscellaneous	Hard X-ray Monitors Torus Pressure Gauges Residual Gas Analyzer Probe Mechanisms

FIGURE CAPTIONS

- Fig. 1. $n\tau$ versus T for tokamak. (Courtesy of H. Furth.)
- Fig. 2. Schematic illustration of a projected CIT ignition pulse. The dashed areas represent possible extensions of the rf power to maximize flexibility.
- Fig. 3. The range in predicted energy confinement times for CIT using a variety of scalings. The length of each box represents the range of predictions using the labeled class of scalings. Approximately 300-340 msec are needed for ignition. Also illustrated is the Q (energy multiplication factor) for a confinement time of ~300 msec.
- Fig. 4. CIT ignition contours ($P_\alpha = P_{Loss}$) and ohmic heating contours ($P_{ohmic} = P_{Loss}$) for neo-Alcator, a typical "L-Mode," and a typical "H-Mode" energy confinement scaling. The Murakami-Hugill density limit of $6.5 \times 10^{20} \text{ m}^{-3}$ and the Troyon beta limits for 9-MA (H-Mode, divertor) and 10-MA (L-Mode, limiter) plasmas are also indicated.
- Fig. 5. Temperature and density profiles for a TFTR discharge several hundred milliseconds after pellet fueling. The pellet has peaked up the central density and cooled the central plasma.²²
- Fig. 6. CIT ignition contours ($P_\alpha = P_{loss}$) and ohmic heating contours for various density profiles [$n = n_0 (1-(r/a)^2)^q$] for L-Mode scaling. The Murakami-Hugill density limit of $6.5 \times 10^{20} \text{ m}^{-3}$ and the Troyon beta limits for a 10-MA limiter discharge are also illustrated.
- Fig. 7. Successive equilibria for two current ramp-up simulations using the TSC code in which the plasma is grown off the inner and outer walls.
- Fig. 8. The electron and ion temperatures and beta's for a CIT simulation for sawtooth periods of 0.25 sec and 0.10 sec. Twenty megawatts of heating is applied for 2 secs and a "H-Mode" confinement model is used. A "soft" beta limit is imposed at the Troyon limit to limit the temperature.
- Fig. 9. Ion temperature profiles (a) for centrally peaked density L-Mode confinement and (b) flat density profiles. Two seconds of 20 MW of off-axis (peaked at $r = 0.5 a$) ICRF heating was provided beginning at $t=0$ in (a) to delay the onset of sawteeth. In (b) 20 MW of centrally-peaked heating was provided for 3.0 secs.
- Fig. 10. Time evolution of the central ion temperature for the two discharges in Fig. 9.

- Fig. 11. The peak and average temperatures, plasma densities, fast-alpha densities, and toroidal beta's calculated as a function of time using "L-Mode" confinement for a 10-MA CIT plasma with a limiter. The "spiky" behavior is due to sawteeth oscillations.
- Fig. 12. The peak and average temperatures, plasma densities, fast-alpha densities, and toroidal beta's calculated as a function of time using "H-Mode" confinement for a 9-MA CIT plasma with a divertor. The "spiky" behavior is due to sawteeth oscillations.
- Fig. 13. Time evolution of the bulk electron and ion temperatures during ^3He minority heating experiments in PLT. 4.3 MW of rf power was absorbed in the plasma center by the resonant ^3He ions at a density of $n_e = 3.7 \times 10^{13} \text{ cm}^{-3}$. Both the background ions and electrons were heated and a strong increase in the sawtooth amplitude was observed.¹³
- Fig. 14. Single pass absorption calculations for (a) pure second harmonic tritium (50-50 D-T plasma at $T = 10 \text{ keV}$, $n_e = 5 \times 10^{14} \text{ cm}^{-3}$) and (b) similar conditions with 5% ^3He minority as functions of the applied parallel wavenumber. The 5% ^3He case indicates the absorption is dominated by the minority species.
- Fig. 15. Calculated equilibrium and vacuum vessel for a TSC calculation of vertical stability. Optional aluminum plates for passive stabilization are shown.
- Fig. 16. Measured radial density scrape-off distances for various tokamak experiments as a function of $(L/B)^{1/2}$.
- Fig. 17. Computational grid for calculating the plasma parameters of the CIT divertor.
- Fig. 18. Calculated contours of neutral density for the CIT divertor.
- Fig. 19. The fraction of the plasma volume that was fueled by a 1.75 mm radius pellet ($\Delta n \leq 10^{14} \text{ cm}^{-3}$) for 5 different velocities (2, 5, 10, 50, and 100 km/sec) as a function of the central electron temperature. This inner half-volume is mixed by sawteeth oscillations.
- Fig. 20. Estimated power balance during a CIT disruption with the given assumptions. The maximum power and energy flux loads to the first wall, limiter, and divertor plates are shown. For a limiter, the dotted box applies.
- Fig. 21. CIT operations plan.

Progress in Toroidal Confinement Parameters

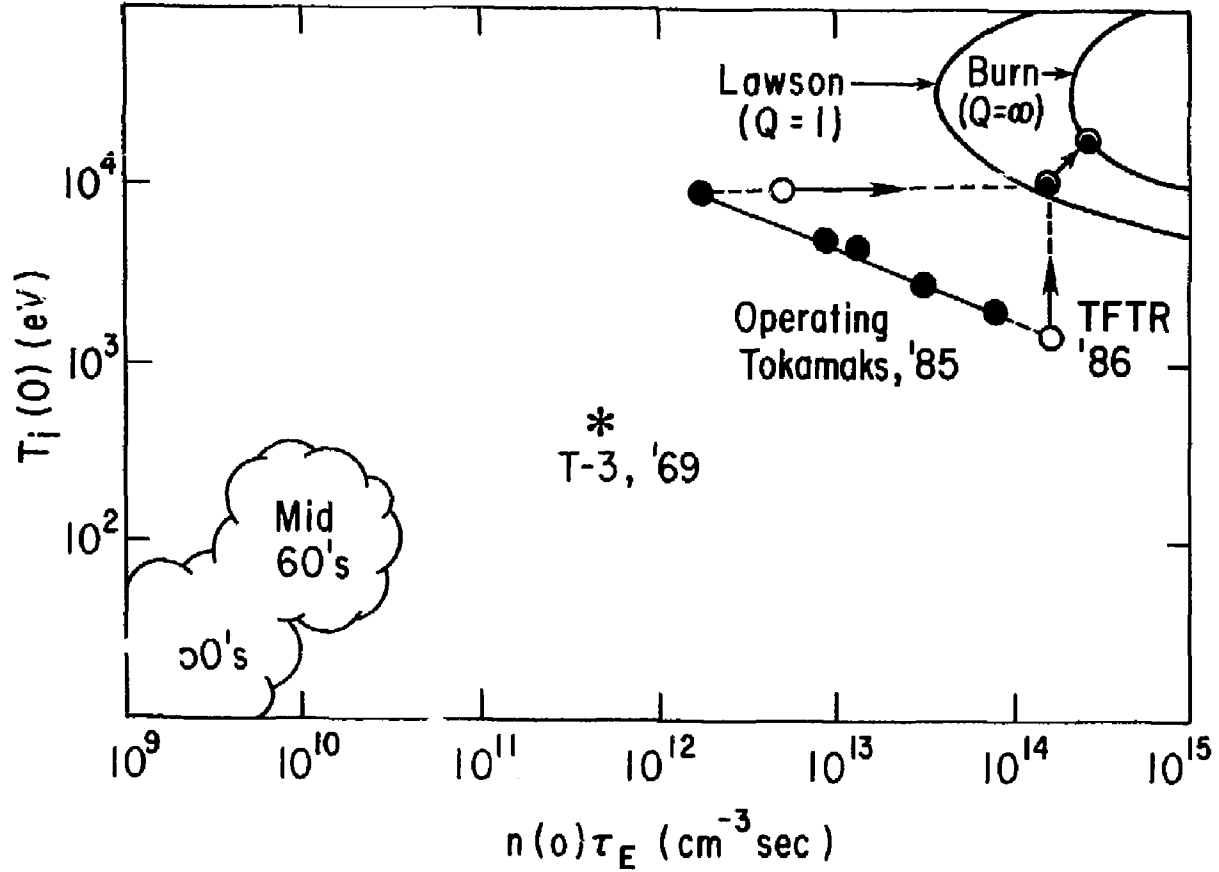


FIG. 1

#86P0104

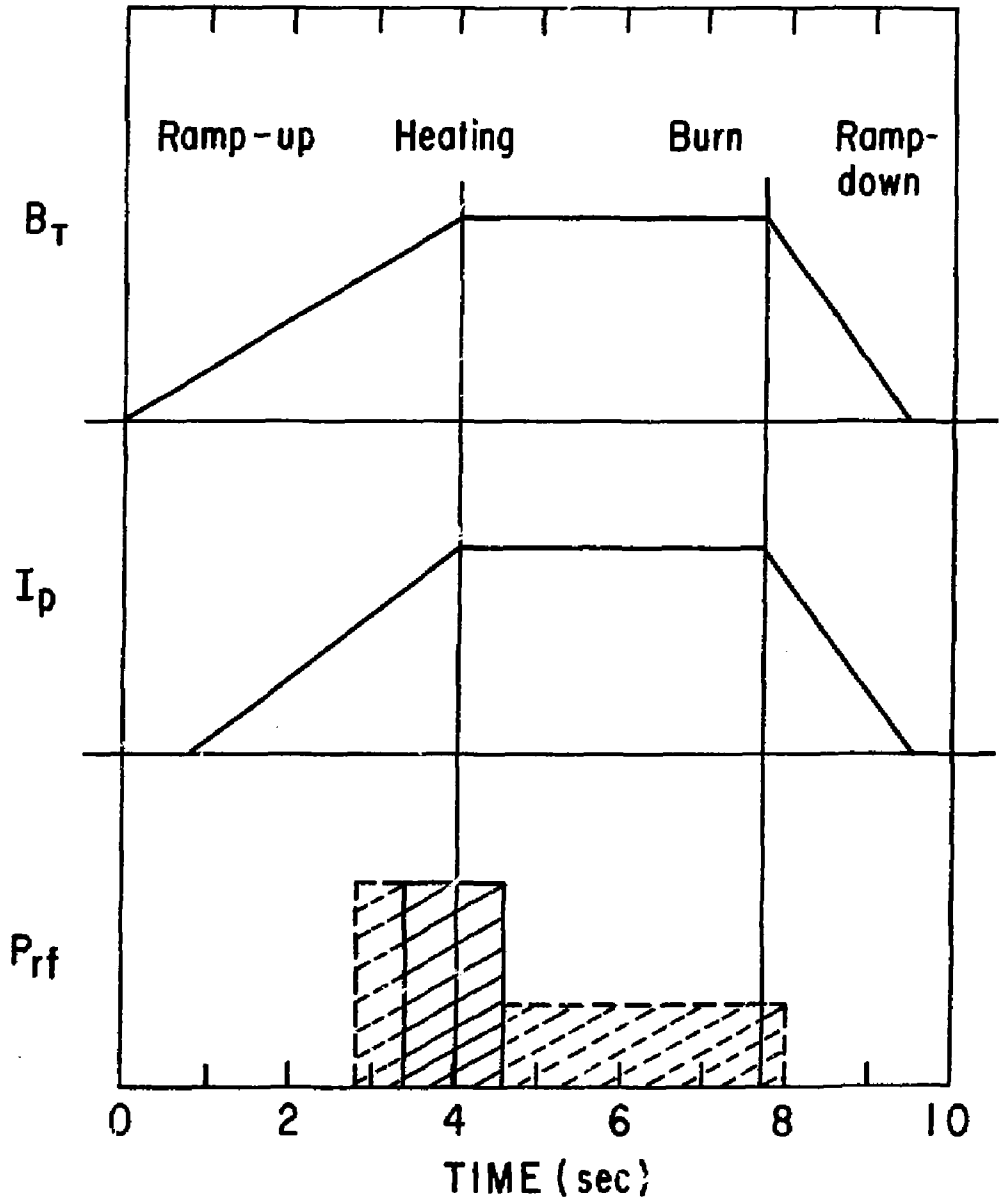


FIG. 2

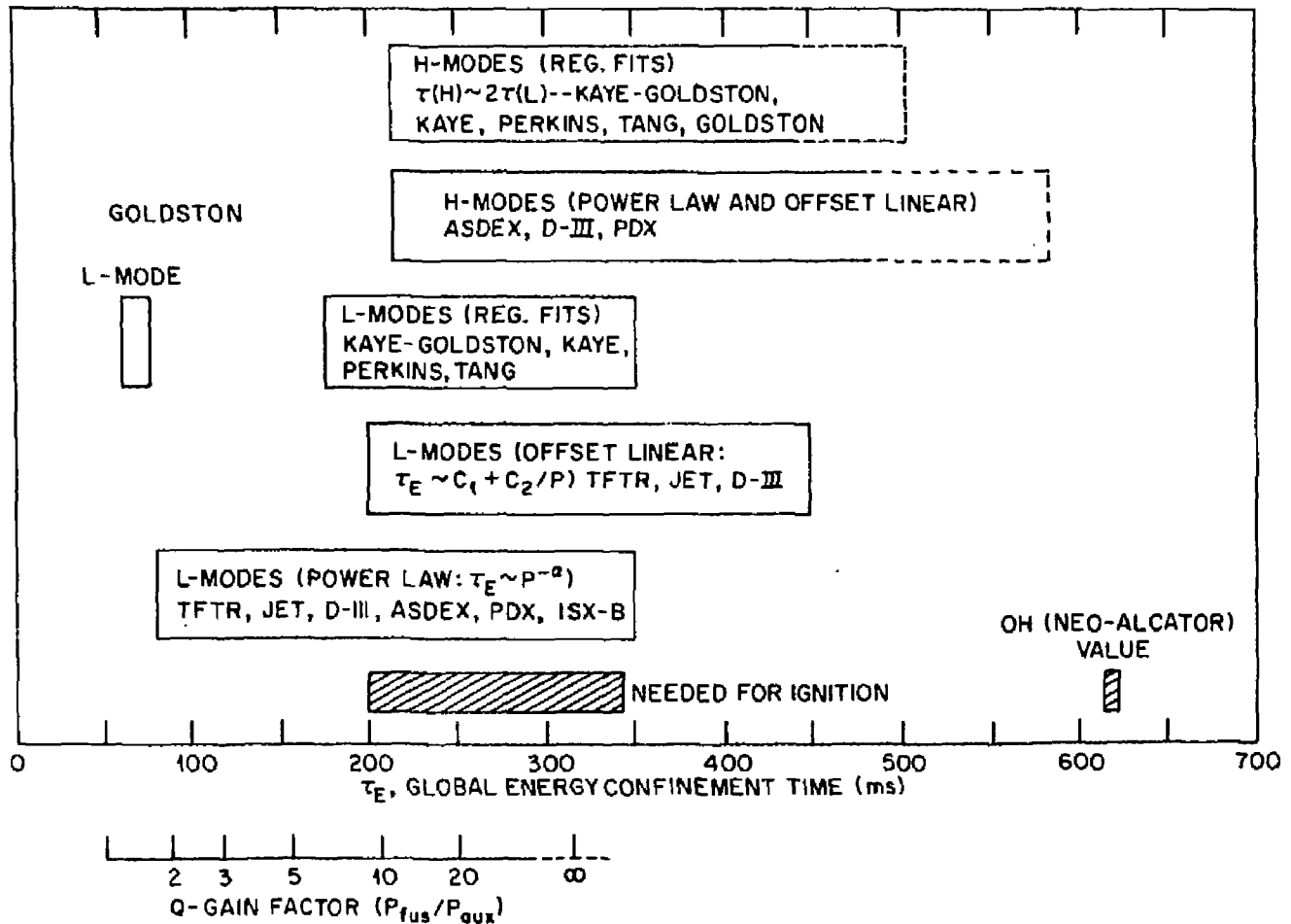


FIG. 3

#86 P0078

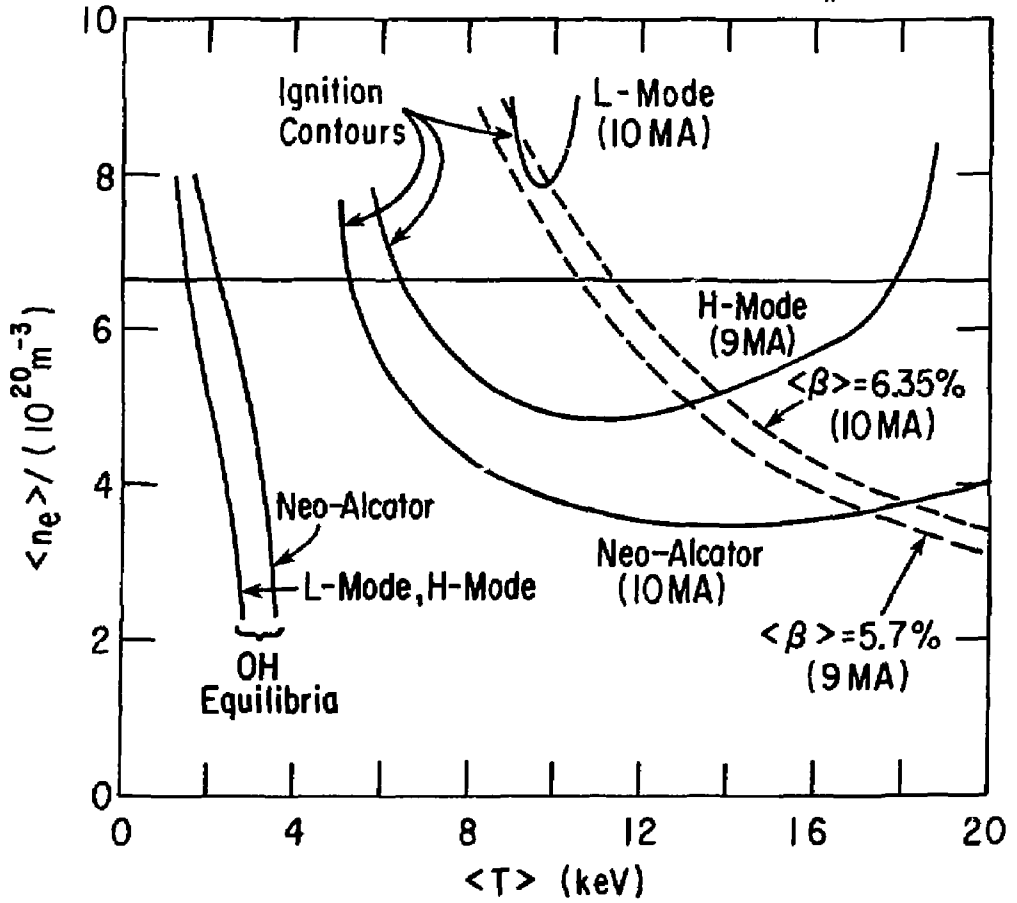


FIG. 4

86P0133

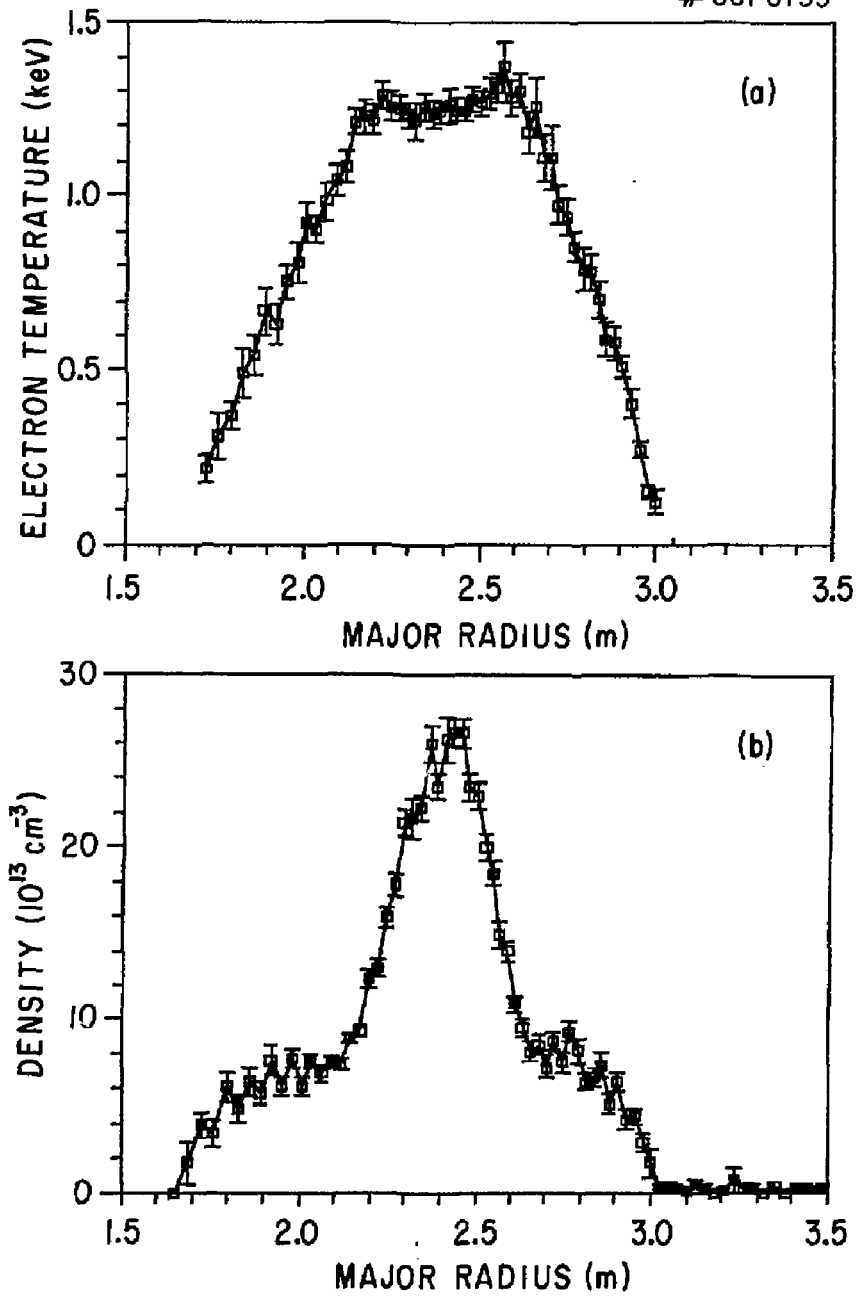


FIG. 5

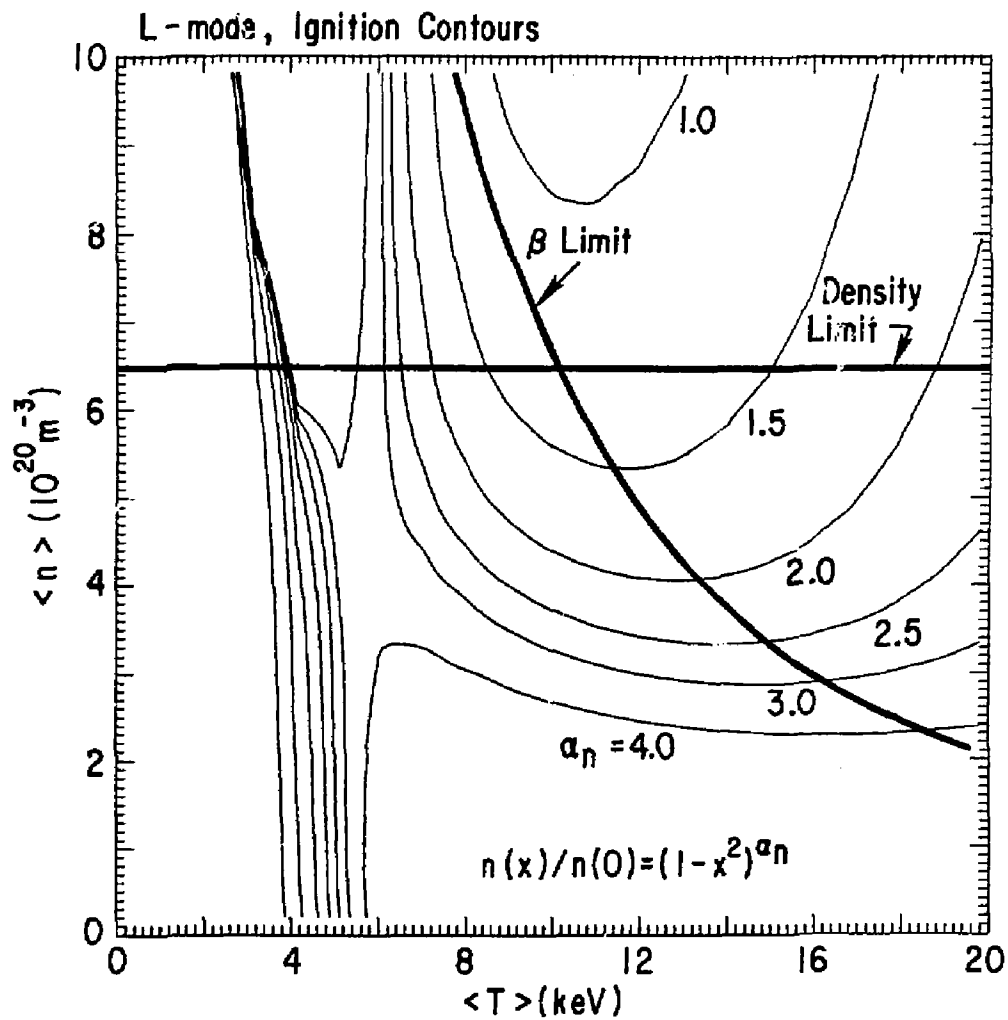


FIG. 6

#86X0714

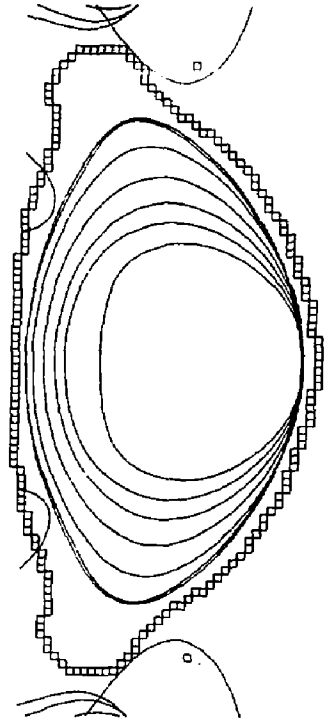
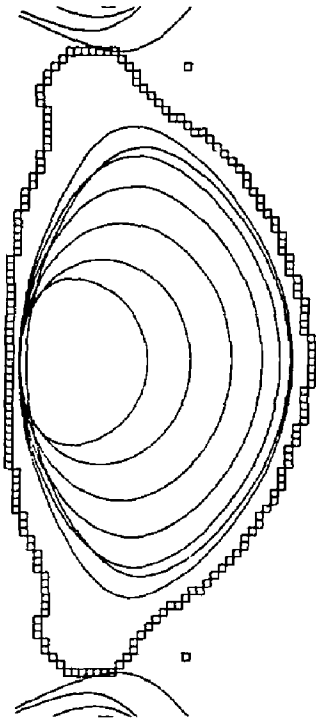


FIG. 7

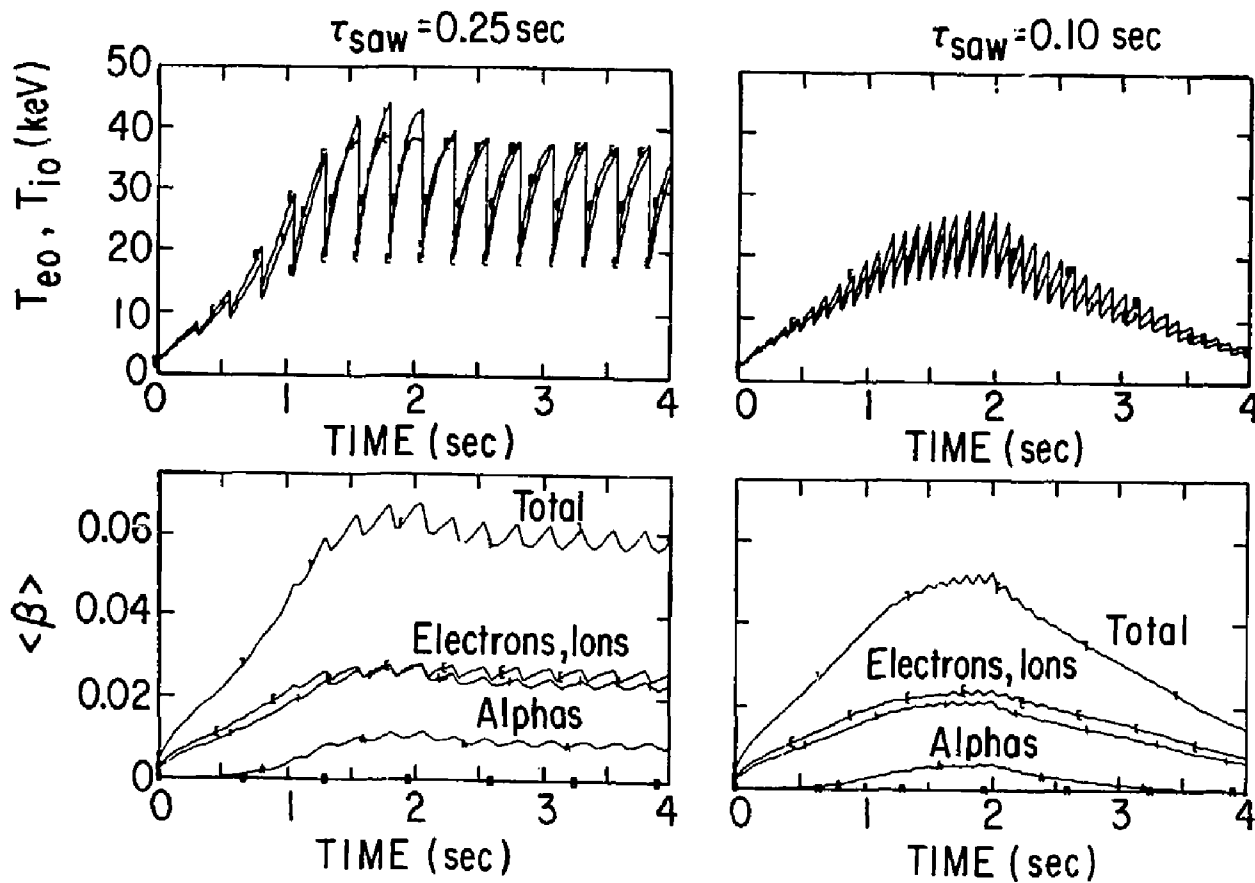
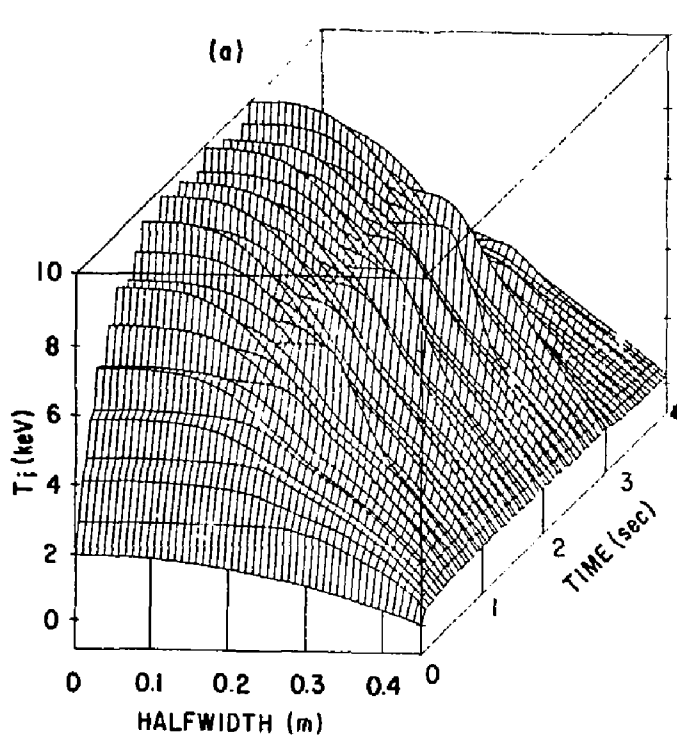
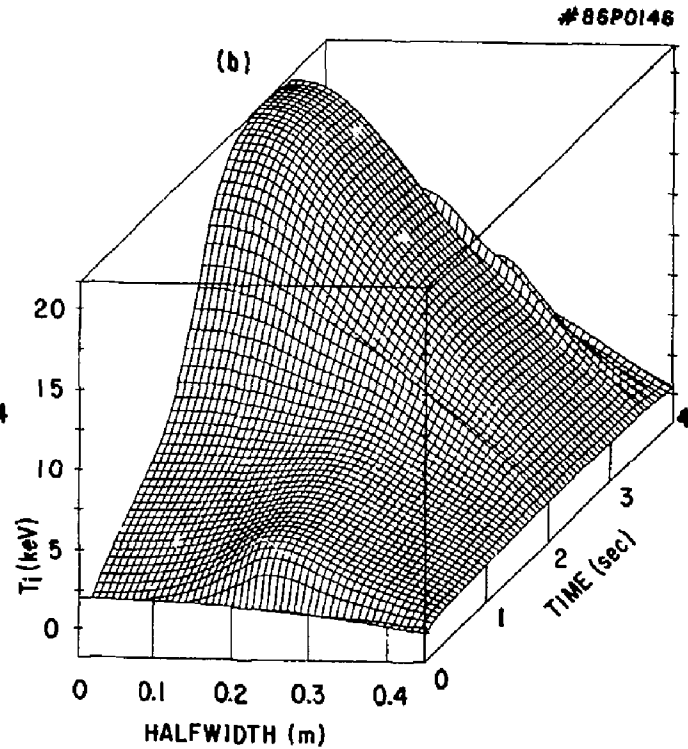


FIG. 8



- Flat Density Profile; Gas Fueling.
- Centrally - Peaked ICRF Heating.



- Peaked Density Profile, Pellet Fuelling.
- Off-Axis ICRF Heating.

FIG. 9

#86P0146

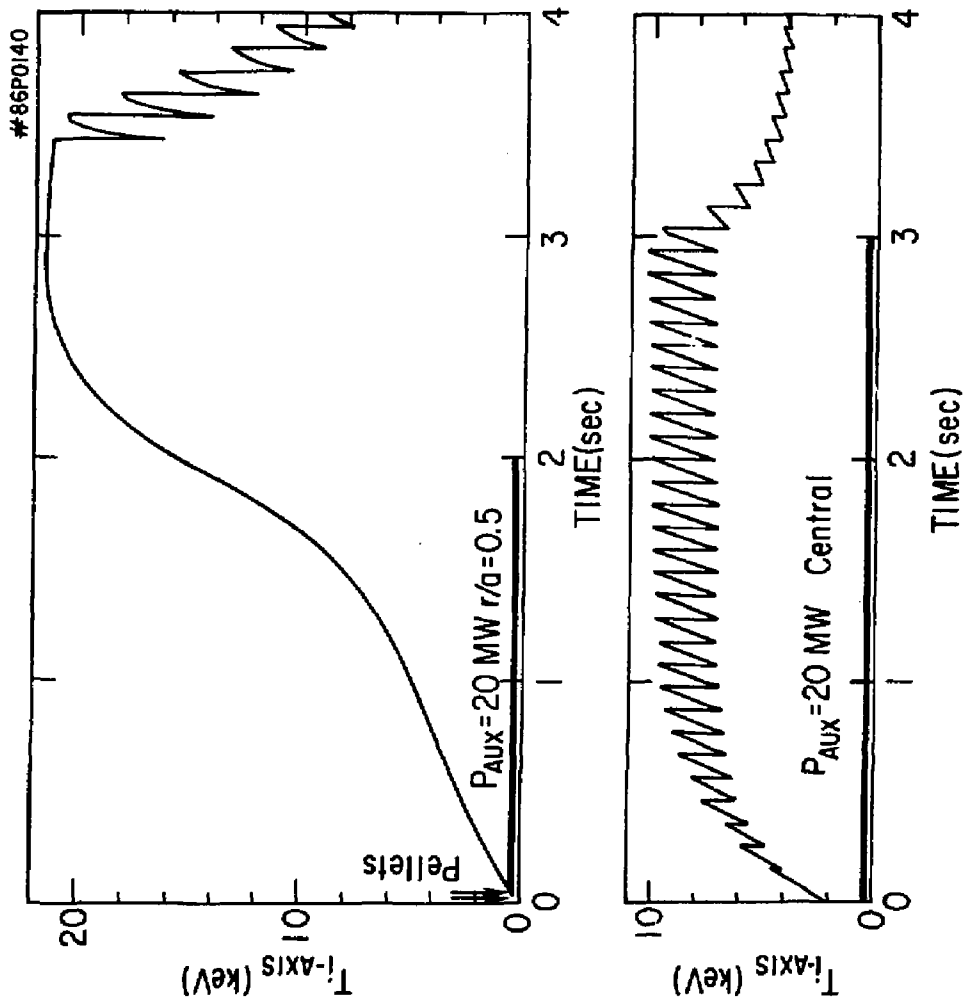


FIG. 10

L-Mode IOVA

#86P0021

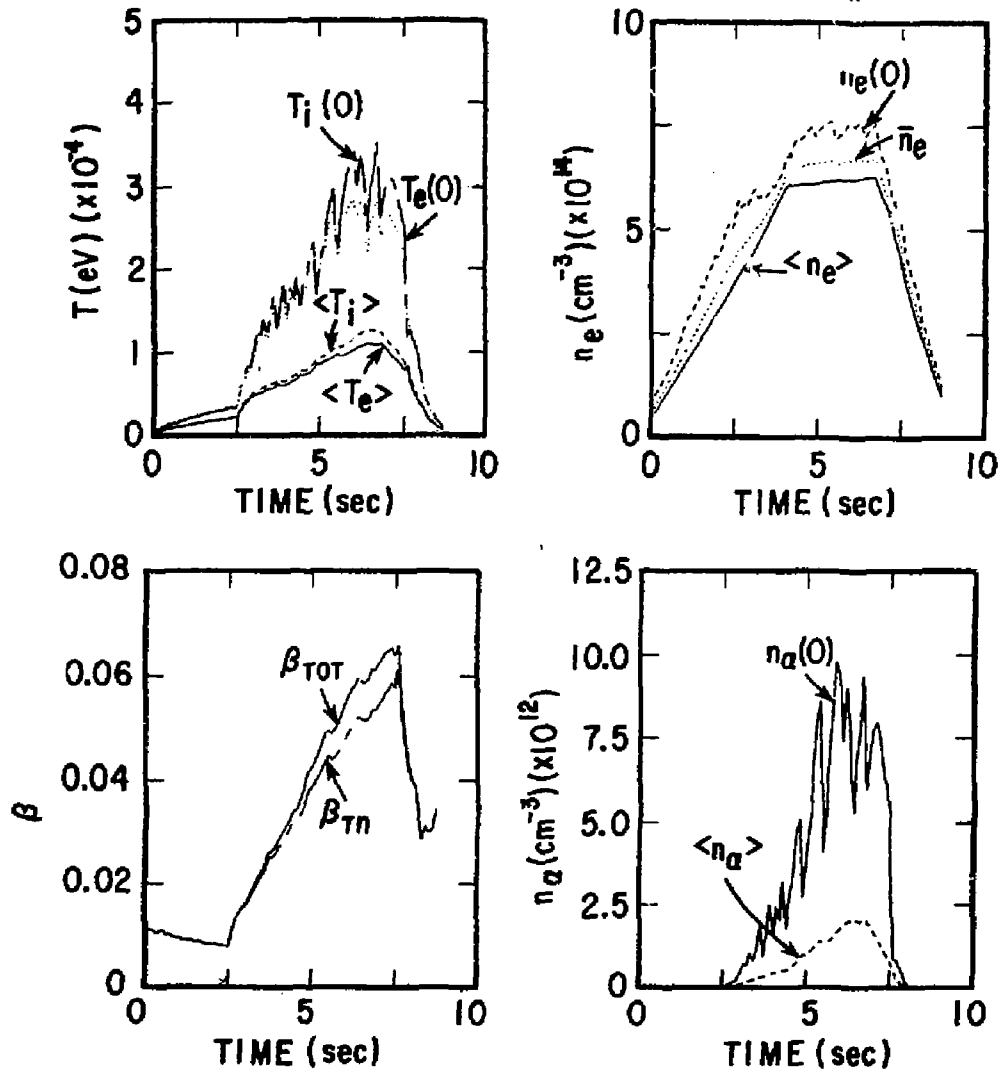


FIG. 11

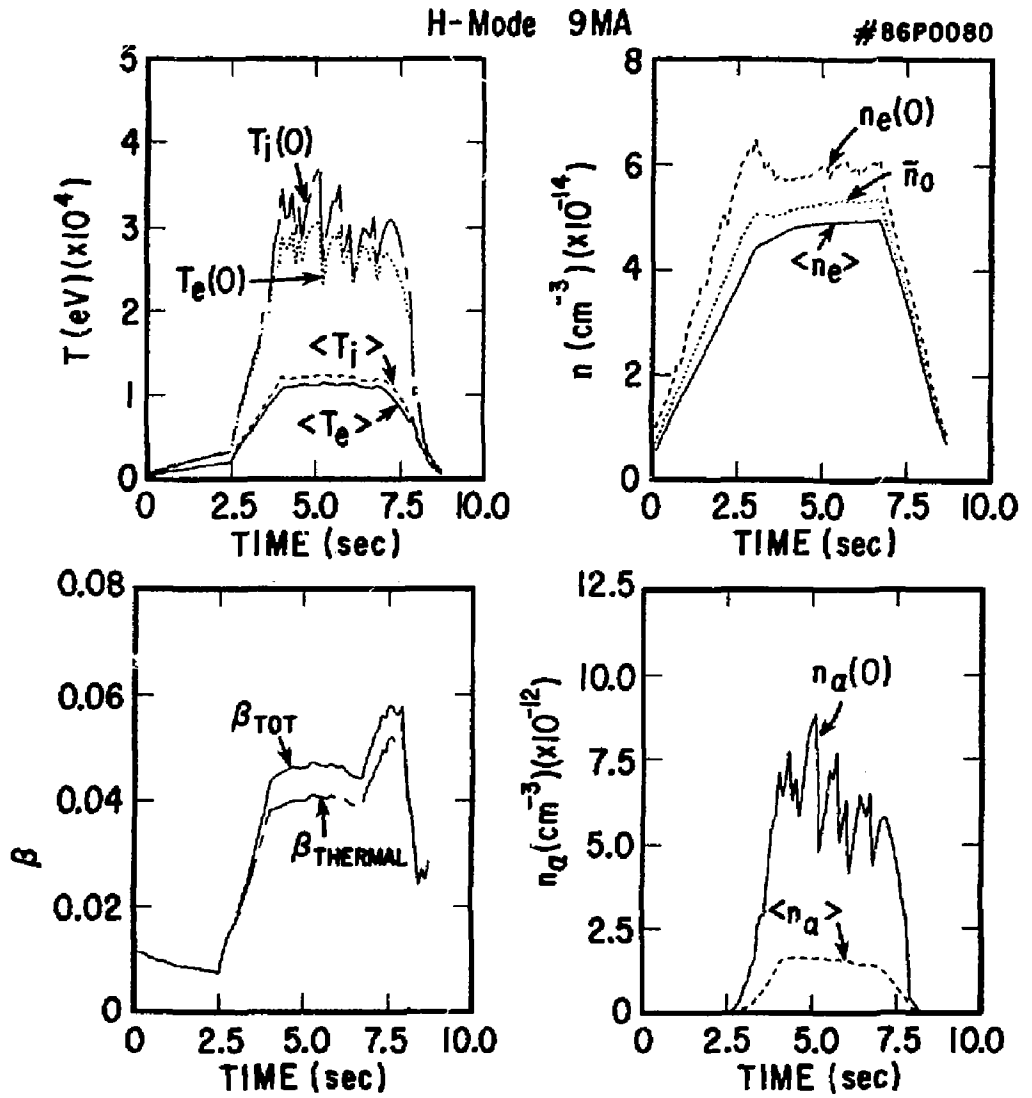


FIG. 12

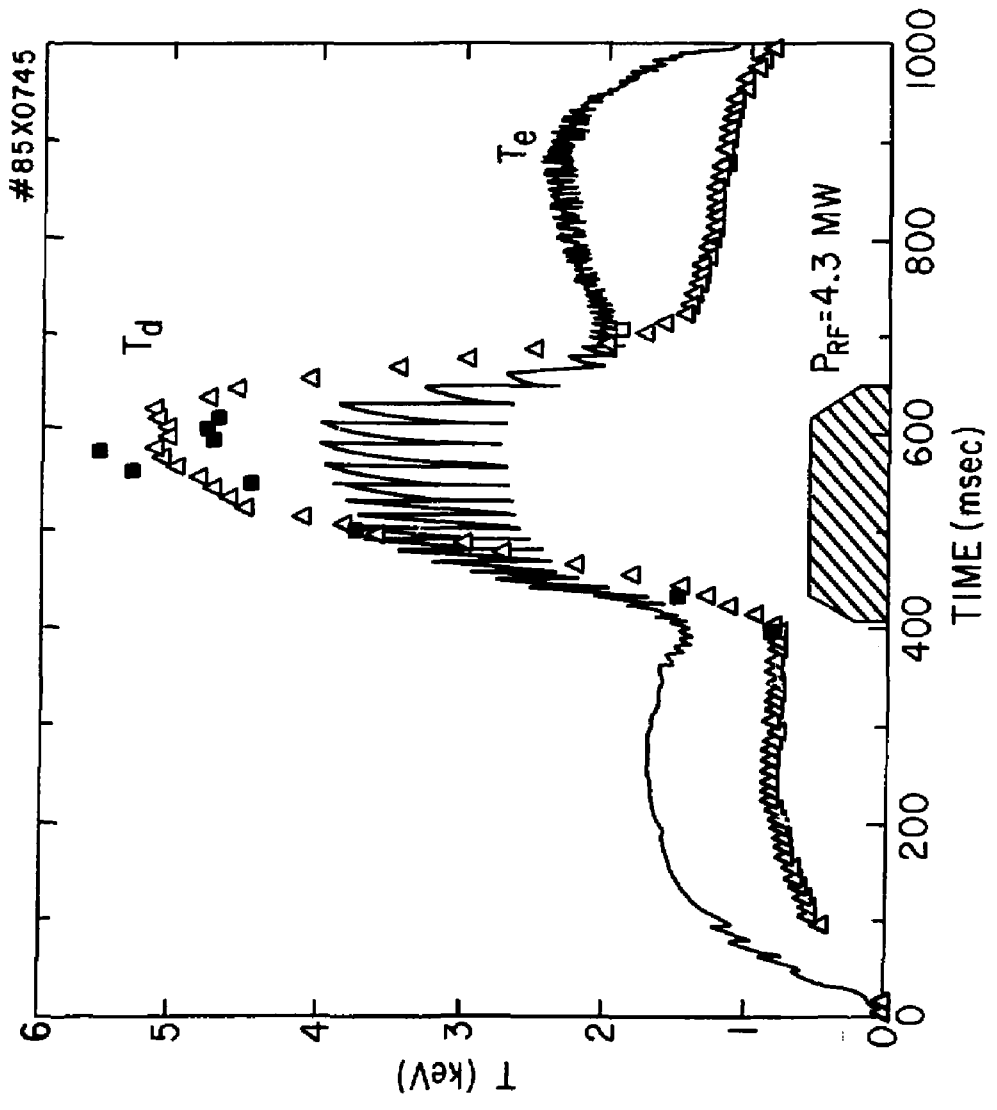


FIG. 13

86X0618

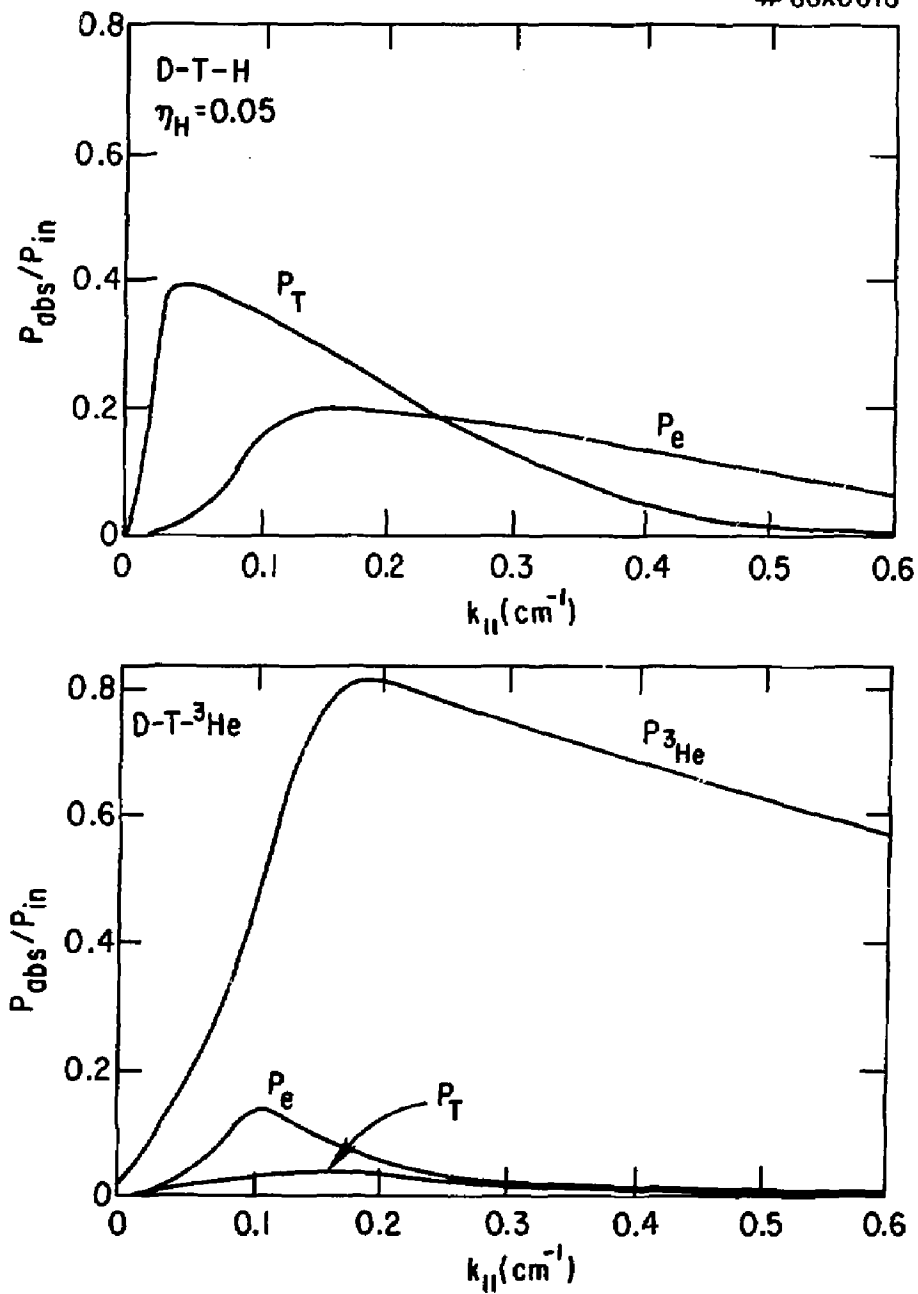


FIG. 14

#86X0713

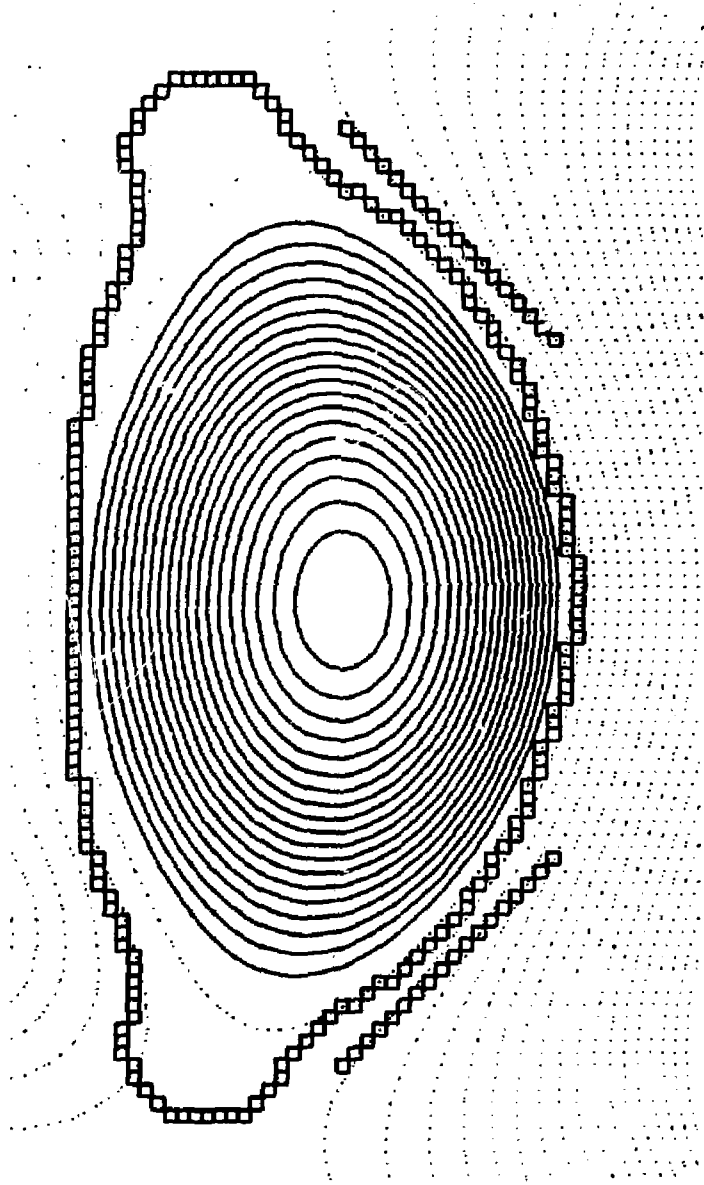


FIG. 15

#86P0075

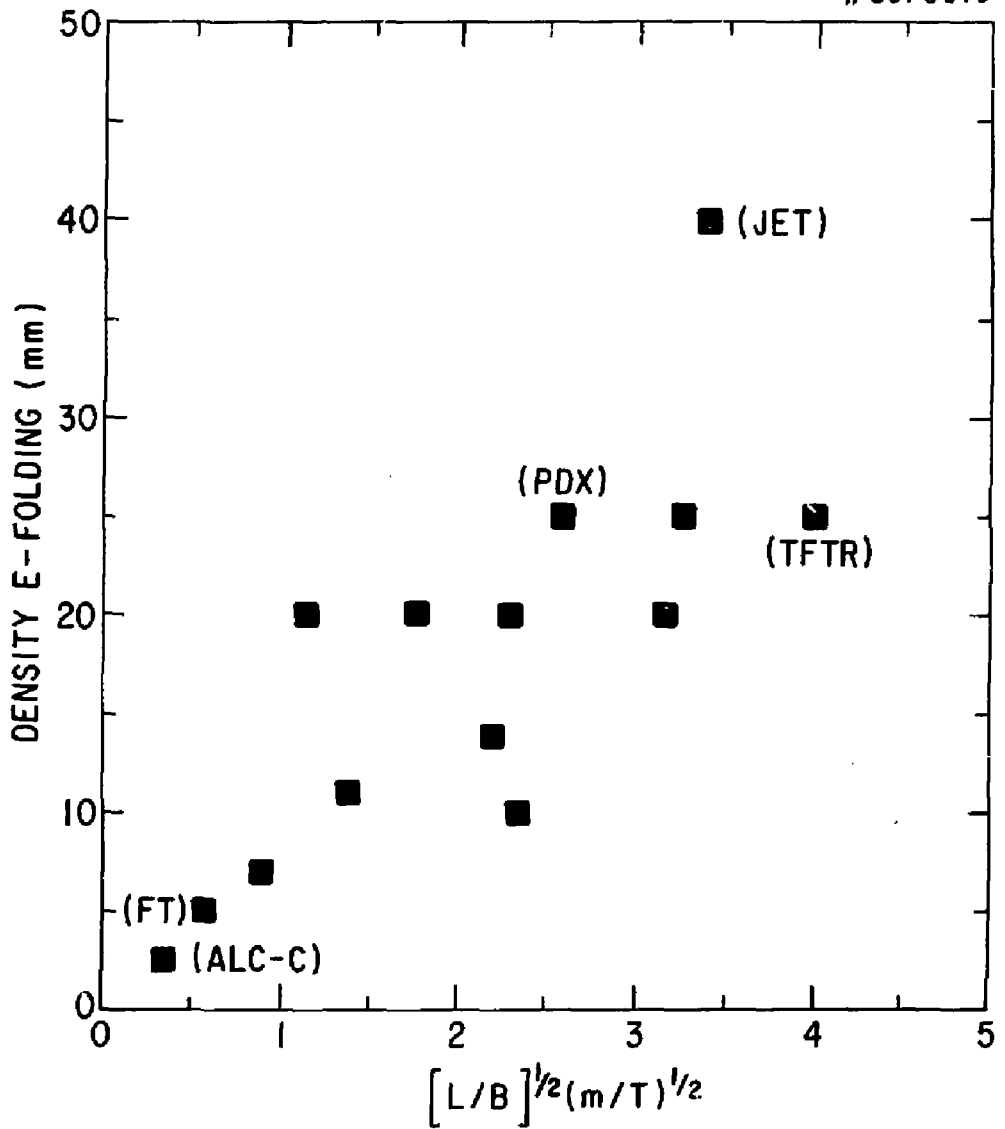


FIG. 16

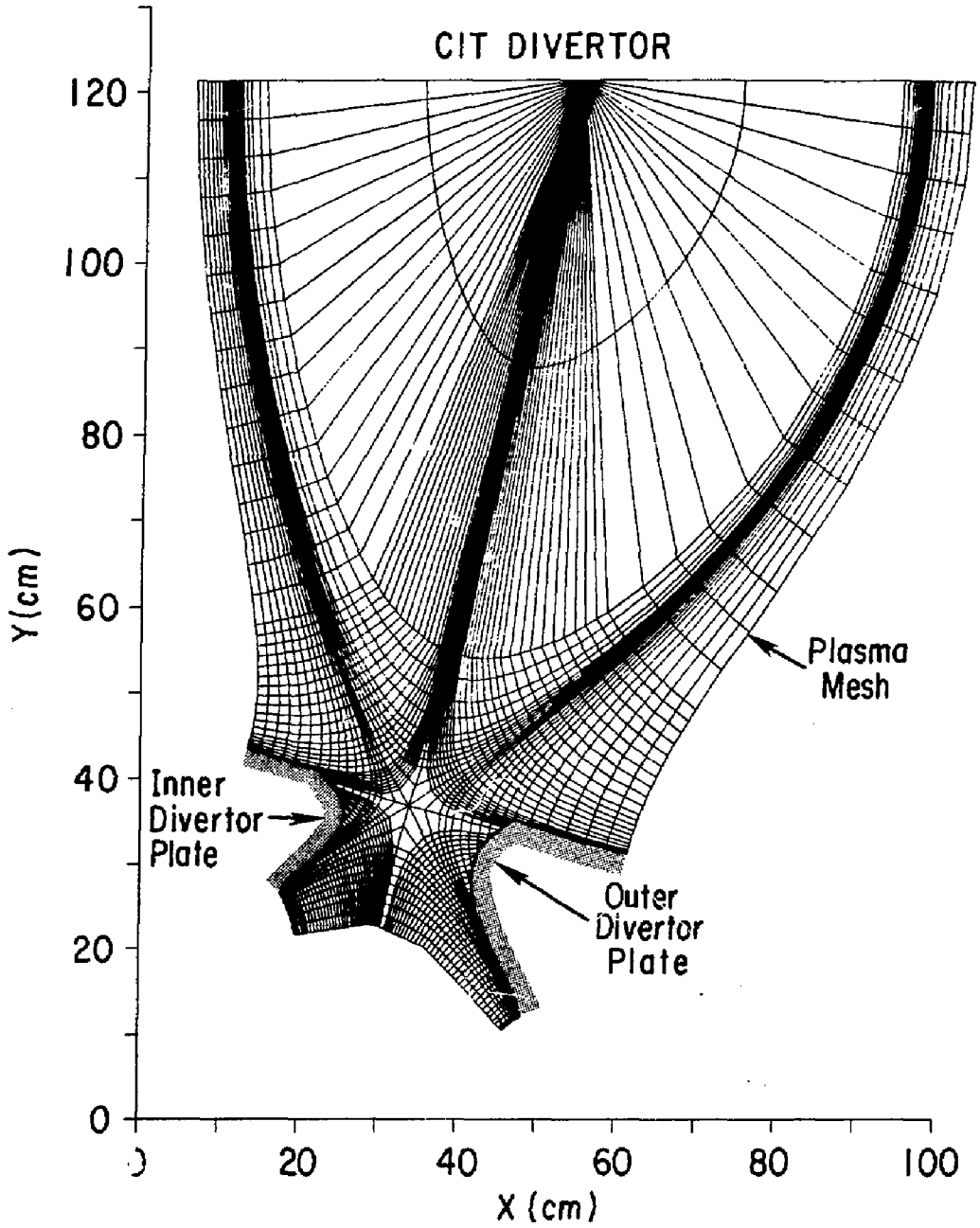


FIG. 17

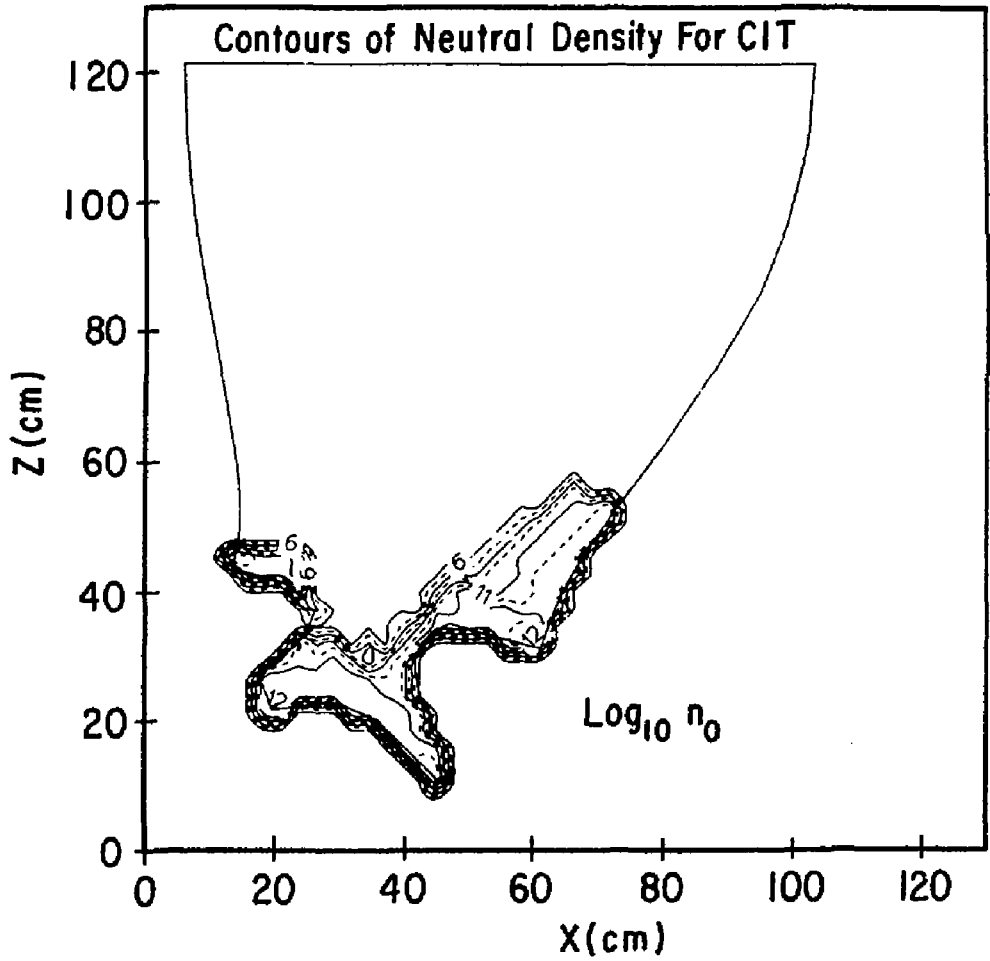


FIG. 18

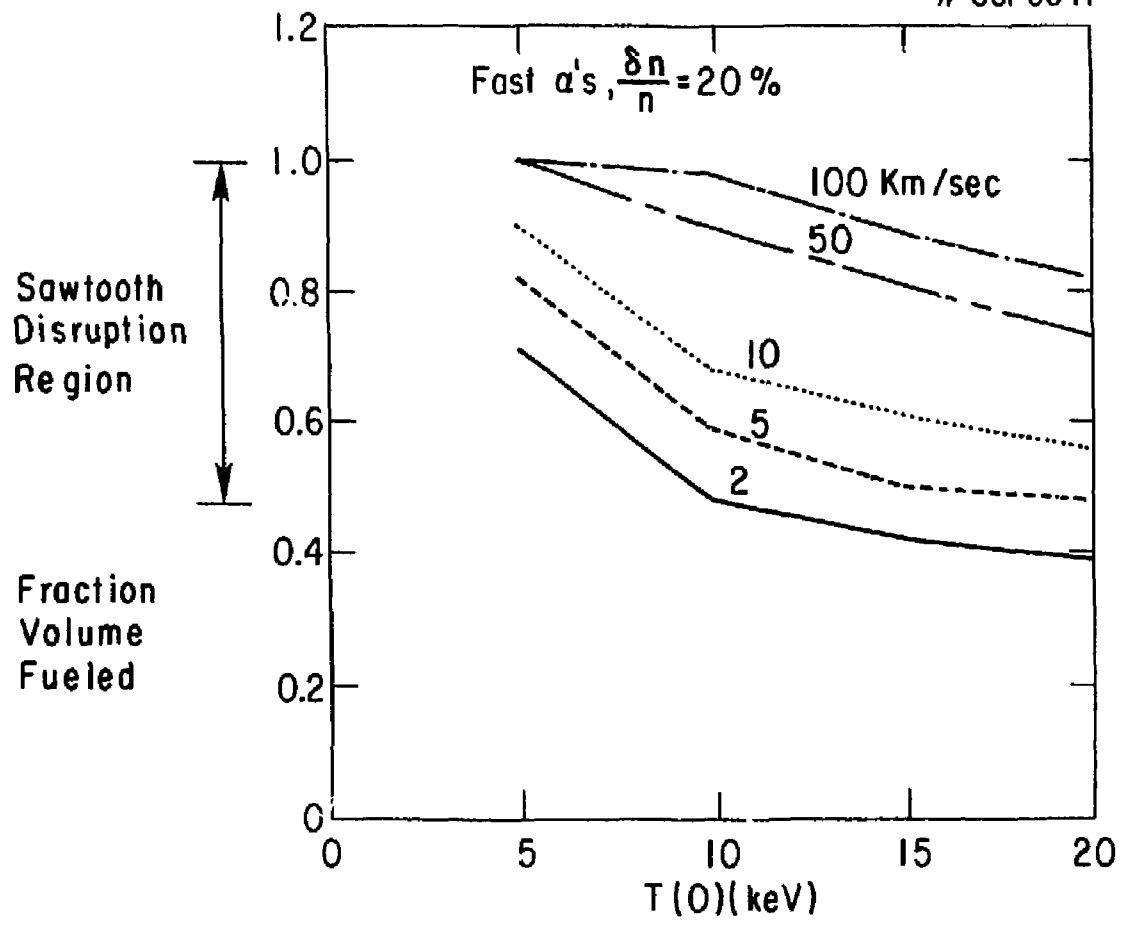


FIG. 19

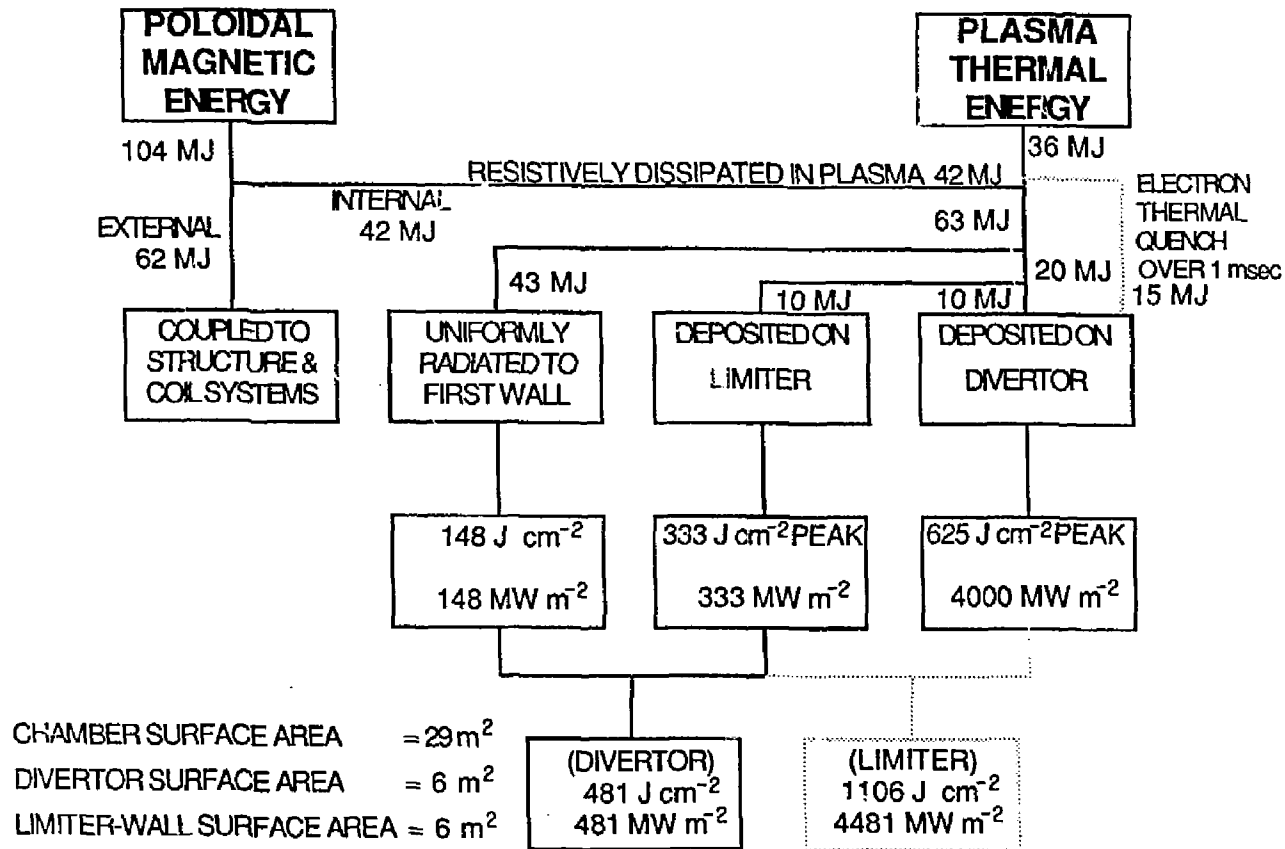
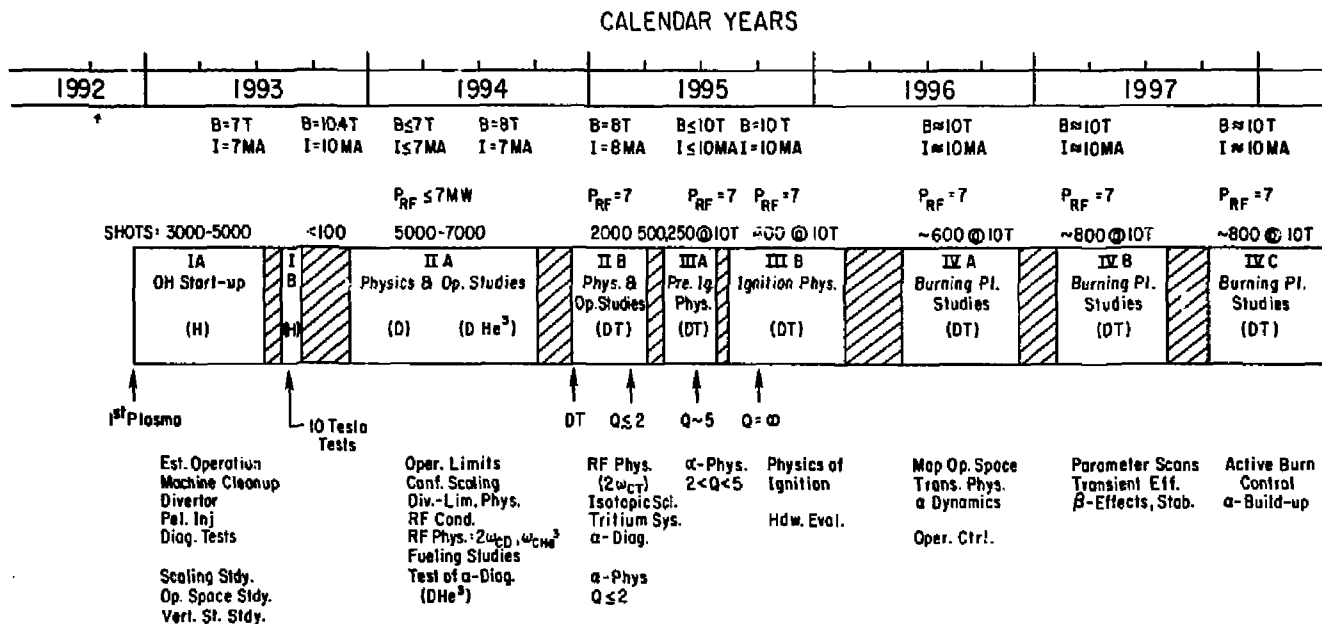


FIG. 20



PROPOSED CIT OPERATIONAL PLAN

FIG. 21

EXTERNAL DISTRIBUTION IN ADDITION TO UC-20

Plasma Res Lab, Austral Nat'l Univ, AUSTRALIA
Dr. Frank J. Paoloni, Univ of Wollongong, AUSTRALIA
Prof. I.R. Jones, Flinders Univ., AUSTRALIA
Prof. M.H. Brennan, Univ Sydney, AUSTRALIA
Prof. F. Cap, Inst Theo Phys, AUSTRIA
M. Goossens, Astronomisch Instituut, BELGIUM
Prof. R. Boucique, Laboratorium voor Natuurkunde, BELGIUM
Dr. D. Palumbo, Dg XII Fusion Prog, BELGIUM
Ecole Royale Militaire, Lab de Phys Plasmas, BELGIUM
Dr. P.H. Sakanaka, Univ Estadual, BRAZIL
Lib. & Doc. Div., Instituto de Pesquisas Espaciais, BRAZIL
Dr. C.R. James, Univ of Alberta, CANADA
Prof. J. Telchmann, Univ of Montreal, CANADA
Dr. H.M. Skarsgard, Univ of Saskatchewan, CANADA
Prof. S.R. Sreenivasan, University of Calgary, CANADA
Prof. Tudor W. Johnston, INRS-Energie, CANADA
Dr. Hannes Barnard, Univ British Columbia, CANADA
Dr. M.P. Bachynski, MPB Technologies, Inc., CANADA
Chalk River, Nucl Lab, CANADA
Zhengwu Li, Sw Inst Physics, CHINA
Library, Tsing Hua University, CHINA
Librarian, Institute of Physics, CHINA
Inst Plasma Phys, Academia Sinica, CHINA
Dr. Peter Lukac, Komenskeho Univ, CZECHOSLOVAKIA
The Librarian, Culham Laboratory, ENGLAND
Prof. Schatzman, Observatoire de Nice, FRANCE
J. Radet, CEN-BP6, FRANCE
JET Reading Room, JET Joint Undertaking, ENGLAND
AM Dupas Library, AM Dupas Library, FRANCE
Dr. Tom Muai, Academy Bibliographic, HONG KONG
Preprint Library, Cent Res Inst Phys, HUNGARY
Dr. R.K. Chhajlani, Vikram Univ, INDIA
Dr. B. Dasgupta, Saha Inst, INDIA
Dr. P. Kew, Physical Research Lab, INDIA
Dr. Phillip Rosenau, Israel Inst Tech, ISRAEL
Prof. S. Cuperman, Tel Aviv University, ISRAEL
Prof. G. Rostagni, Univ Di Padova, ITALY
Librarian, Int'l Ctr Theo Phys, ITALY
Miss Clotia De Palo, Assoc EURATOM-ENEA, ITALY
Biblioteca, del CNR EURATOM, ITALY
Dr. H. Yamato, Toshiba Res & Dev, JAPAN
Direc. Dept. Lg. Tokamak Dev. JAERI, JAPAN
Prof. Nobuyuki Inoue, University of Tokyo, JAPAN
Research Info Center, Nagoya University, JAPAN
Prof. Kyoji Nishikawa, Univ of Hiroshima, JAPAN
Prof. Sigeru Mori, JAERI, JAPAN
Prof. S. Tanaka, Kyoto University, JAPAN
Library, Kyoto University, JAPAN
Prof. Ichiro Kawakami, Nihon Univ, JAPAN
Prof. Satoshi Itoh, Kyushu University, JAPAN
Dr. D.I. Choi, Adv. Inst Sci & Tech, KOREA
Tech Info Division, KAERI, KOREA
Bibliotheek, Fom-Inst Voor Plasma, NETHERLANDS
Prof. B.S. Lilley, University of Waikato, NEW ZEALAND
Prof. J.A.C. Cabral, Inst Superior Tecn, PORTUGAL
Dr. Octavian Petrus, ALI CLZA University, ROMANIA
Prof. M.A. Hellberg, University of Natal, SO AFRICA
Dr. Johan de Villiers, Plasma Physics, Nucor, SO AFRICA
Fusion Div, Library, JEN, SPAIN
Prof. Hans Wilhelmson, Chalmers Univ Tech, SWEDEN
Dr. Lennart Stenflo, University of UMEA, SWEDEN
Library, Royal Inst Tech, SWEDEN
Centre de Recherches, Ecole Polytech Fed, SWITZERLAND
Dr. V.T. Tolok, Kharkov Phys Tech Ins, USSR
Dr. D.D. Ryutov, Siberian Acad Sci, USSR
Dr. G.A. Eiliseev, Kurchatov Institute, USSR
Dr. V.A. Glukhikh, Inst Electro-Physical, USSR
Institute Gen. Physics, USSR
Prof. T.J.M. Boyd, Univ College N Wales, WALES
Dr. K. Schindler, Ruhr Universitat, W. GERMANY
ASDEX Reading Rm, IPP/Max-Planck-Institut fur
Plasmaphysik, F.R.G.
Nuclear Res Estab, Julich Ltd, W. GERMANY
Librarian, Max-Planck Institut, W. GERMANY
Bibliothek, Inst Plasmaforschung, W. GERMANY
Prof. R.K. Janev, Inst Phys, YUGOSLAVIA